

Optimizing Phase Contrast in TEM by the use of an electrostatic Boersch Phase Plate

R.R. Schröder¹⁾, B. Barton¹⁾, K. Schultheiss²⁾,
D. Gerthsen²⁾

1) Max-Planck-Institute of Biophysics, Max-von-Laue Str. 3, D-60438
Frankfurt/Main, Germany

2) Laboratorium für Elektronenmikroskopie and Center for Functional
Nanostructures (CFN), Universität Karlsruhe (TH), D-76128 Karlsruhe,
Germany

Fabian Pérez-Willard

University of Karlsruhe, Zeiss-NTS

Endre Majorovits

MPI Med. Research / University Oxford

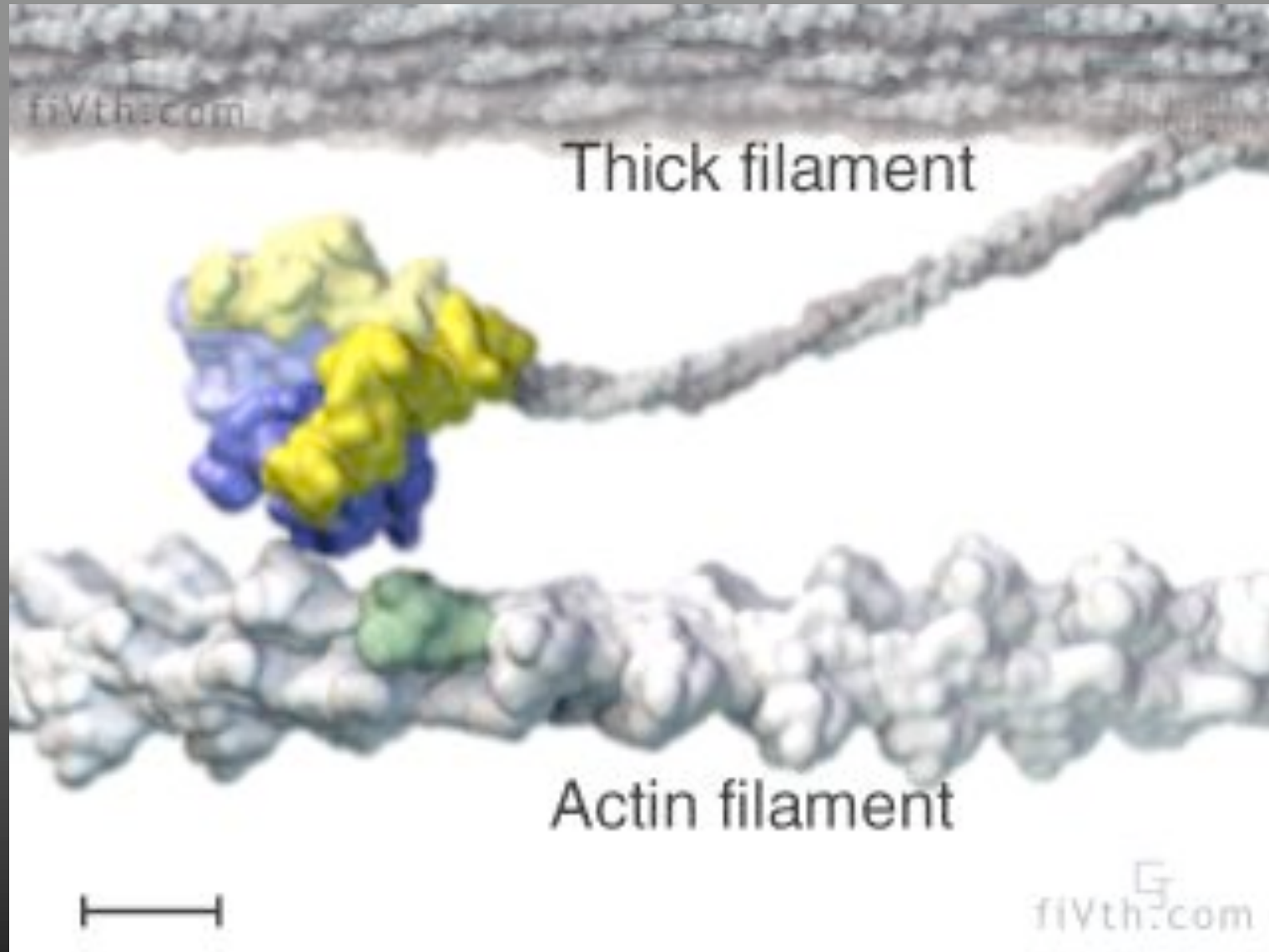
Radostin Danev

NIPS, Okazaki University

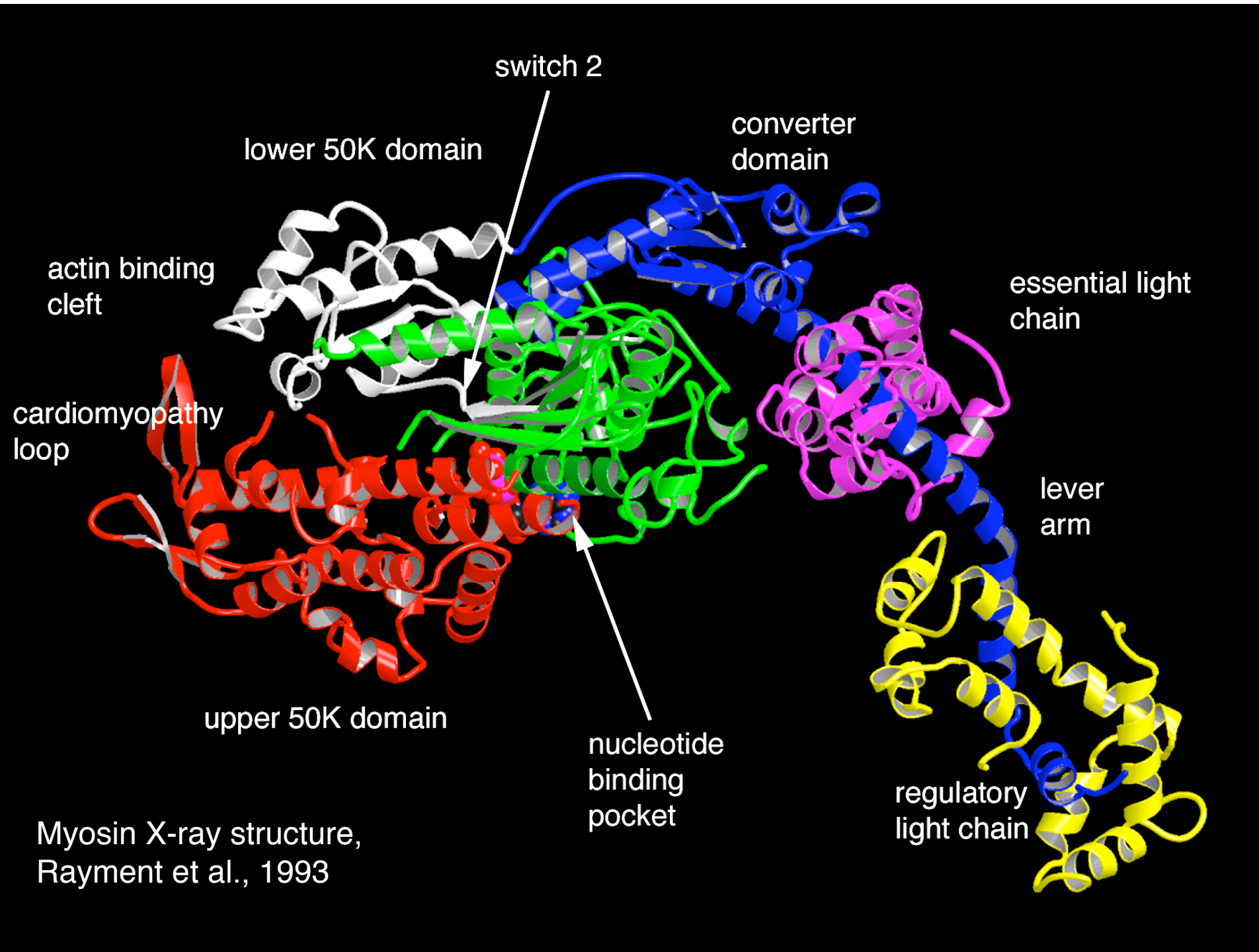
Kuniaki Nagayama

Werner Kühlbrandt

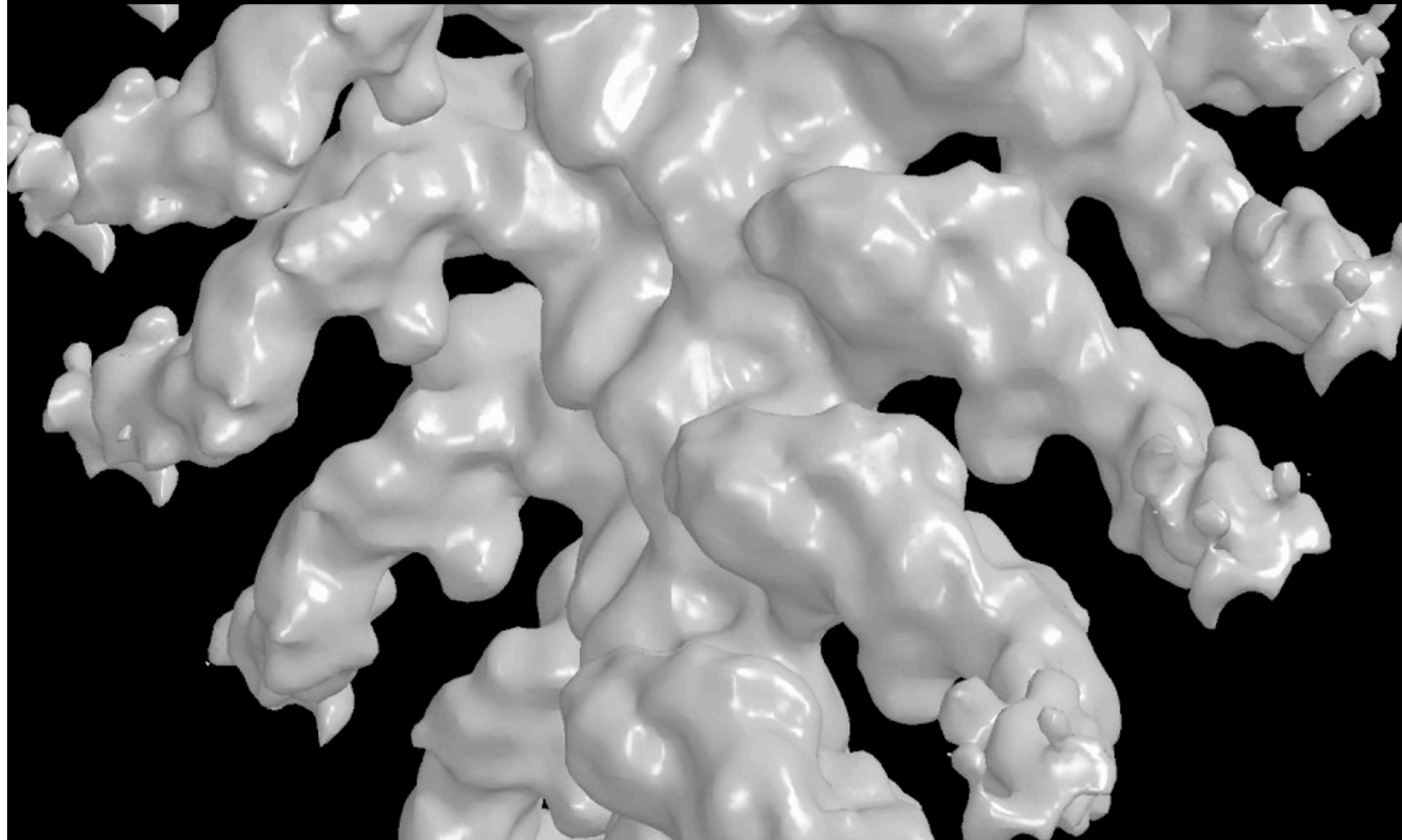
MPI Biophysics, Frankfurt/Main

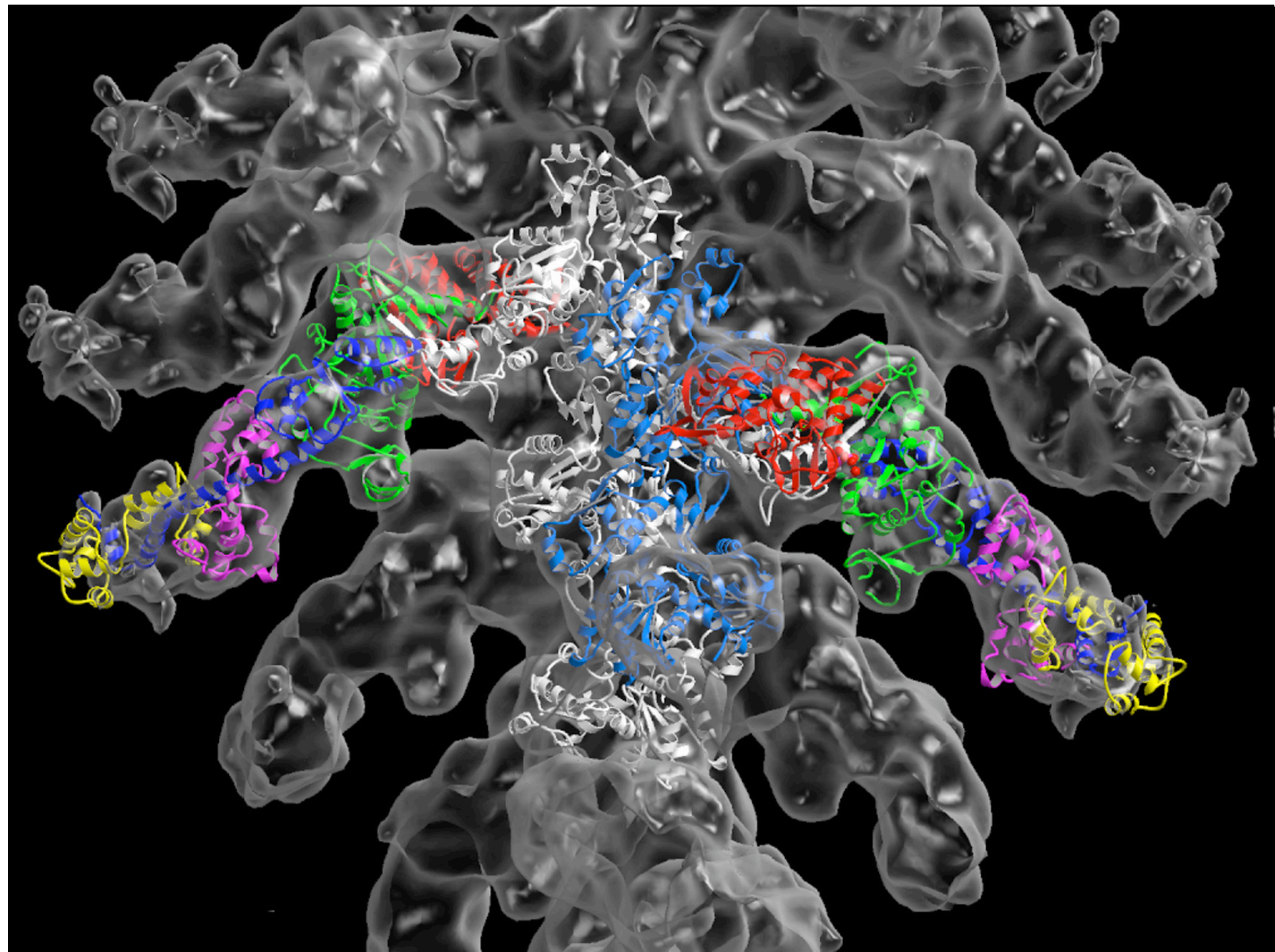


“How muscle works ...”, from Ron Vales’s web page



**Reconstruction of the rigor actin-myosin complex
(chicken skeletal myosin II papain S1, Holmes et al., 2003)**
Resolution 13-15Å (Fourier shell coefficients)

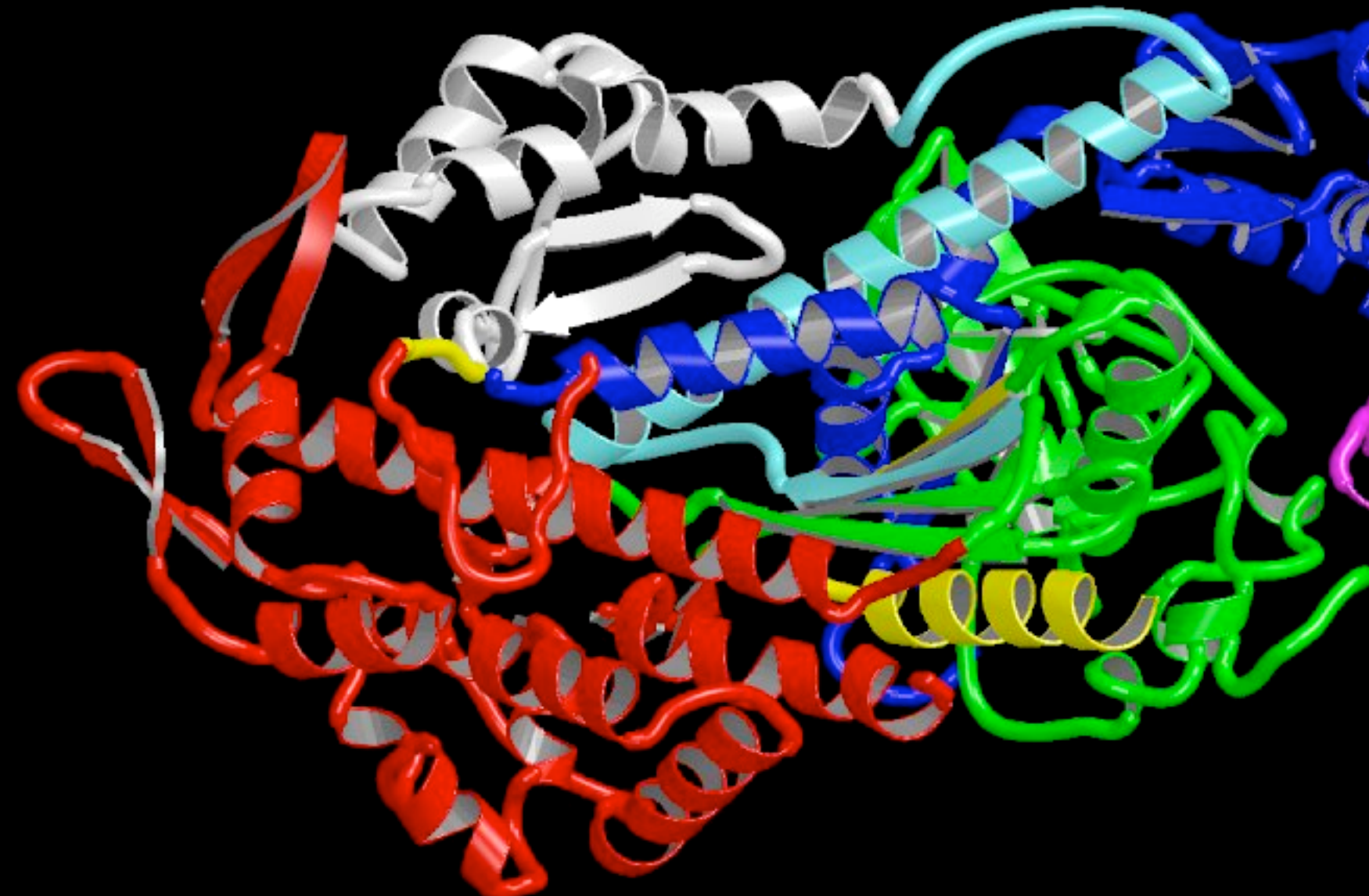


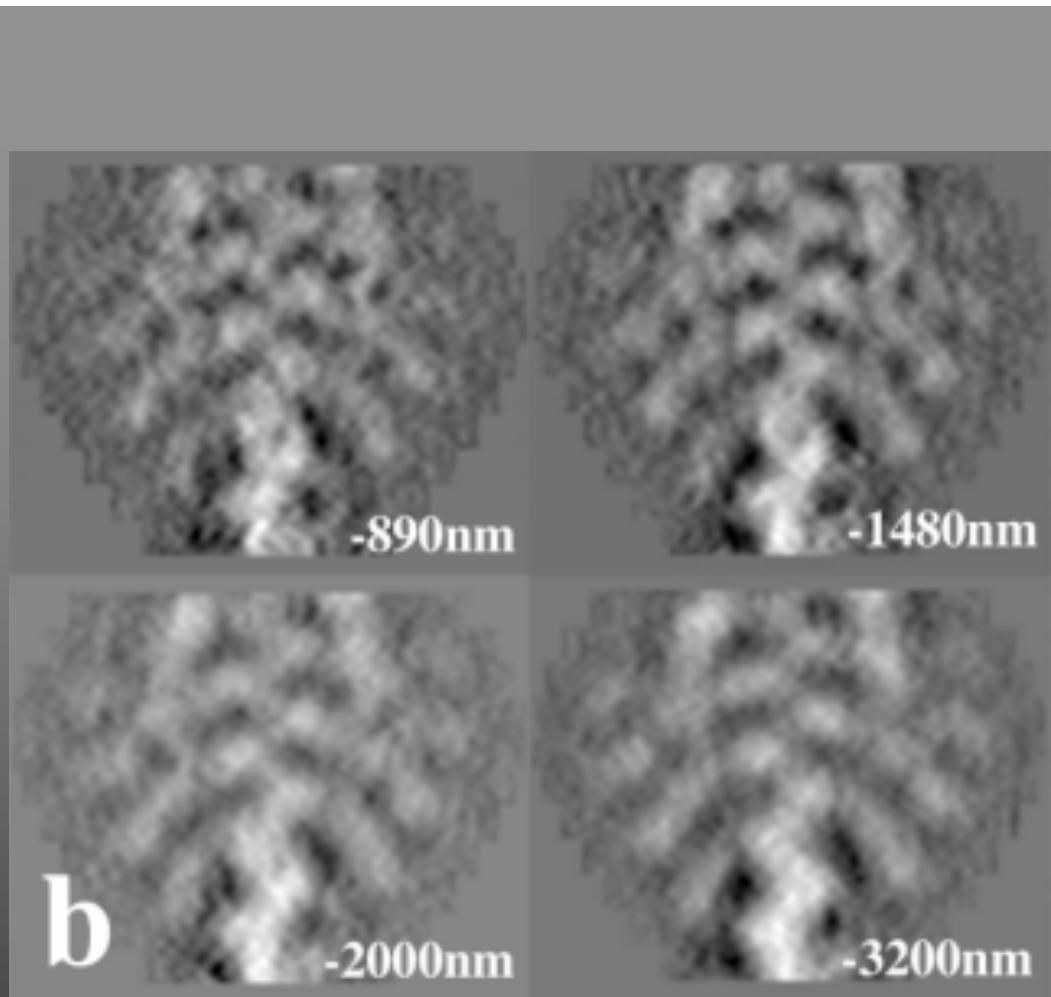
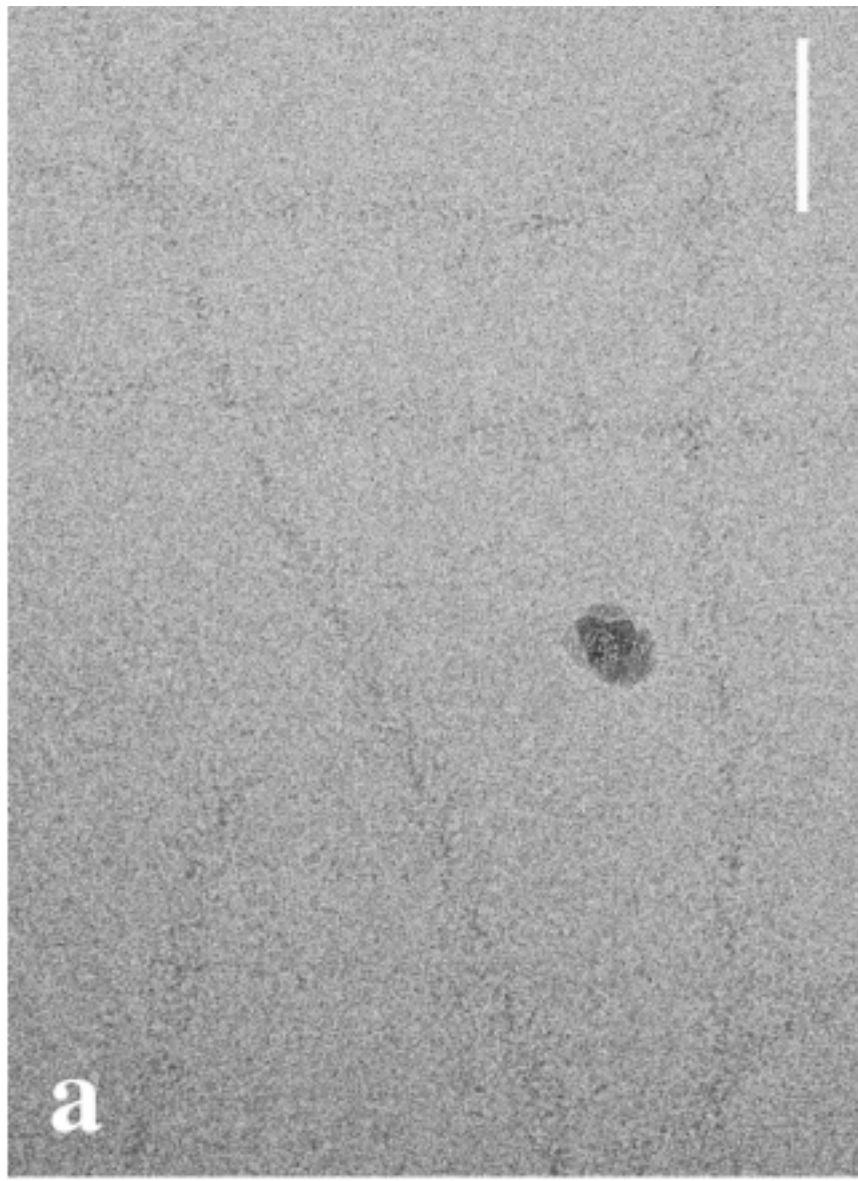


chicken skeletal



upper/lower 50K free





a - a typical sample of decorated actin at an underfocus of 1.48 μm . (scale bar 77 nm)

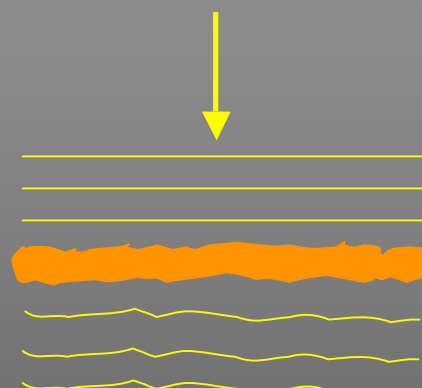
b – averages of 104 identical object areas selected from the four exposures in one defocus series. Half a 38.5 nm repeat is shown for each underfocus exposure

Outline

- Phase contrast in transmission electron microscopy
- Why an electrostatic phase plate?
- The design of a Boersch-type electrostatic phase plate
- First experimental results
- The future

Phase Contrast in Electron Microscopy

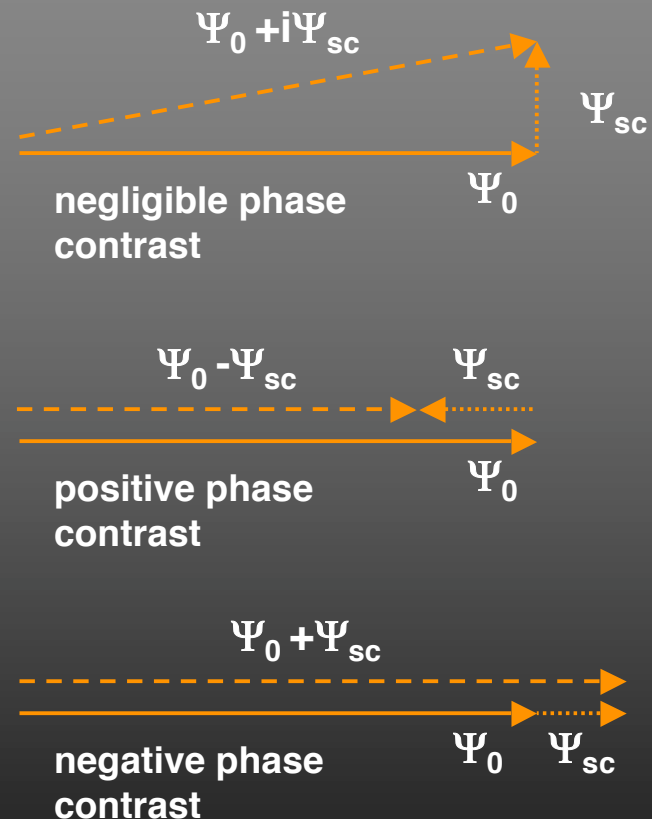
e^-



biological
sample: weak
phase object
(H, N, C, O, S ...)

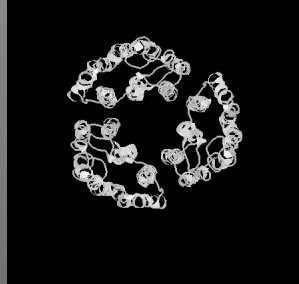
weak phase object

- $\pi/2$ -phase shift due to elastic scattering + small scattering amplitude (1st order Born approximation)
- negligible phase contrast
- low object signal

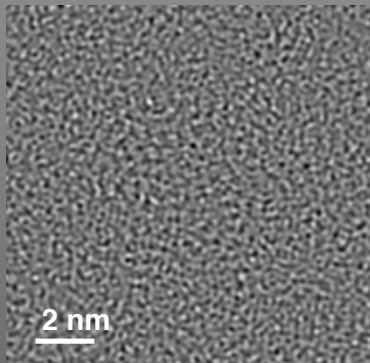


Simulation of bacterio rhodopson (bR) without/with Phase Plate

without phase plate

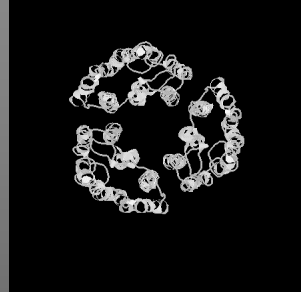


200 keV
 $C_s = 2.7 \text{ mm}$
focus

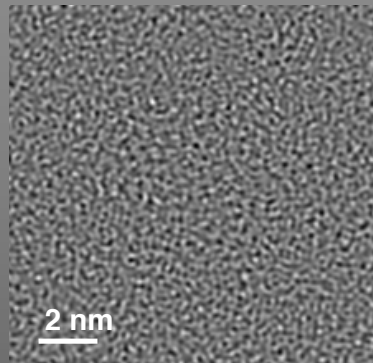


Simulation of bacterio rhodopson (bR) without/with Phase Plate

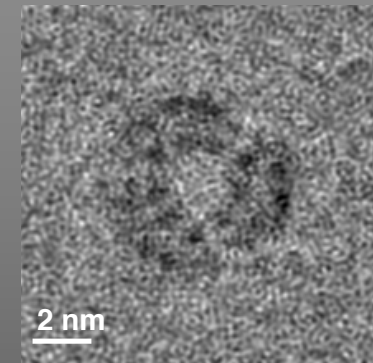
without phase plate



200 keV
 $C_s = 2.7 \text{ mm}$
focus



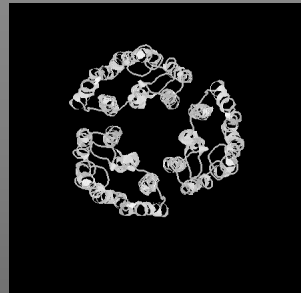
with phase plate



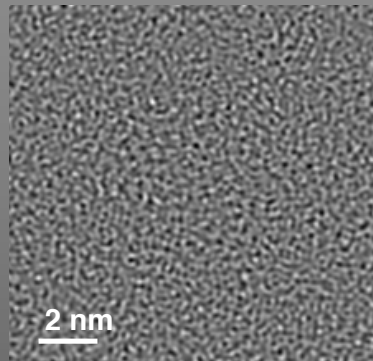
$\pi/2$ -phase shift
→
phase plate

Simulation of bacterio rhodopson (bR) without/with Phase Plate

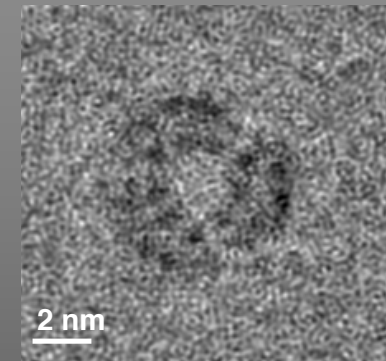
without phase plate



200 keV
 $C_s = 2.7 \text{ mm}$
focus

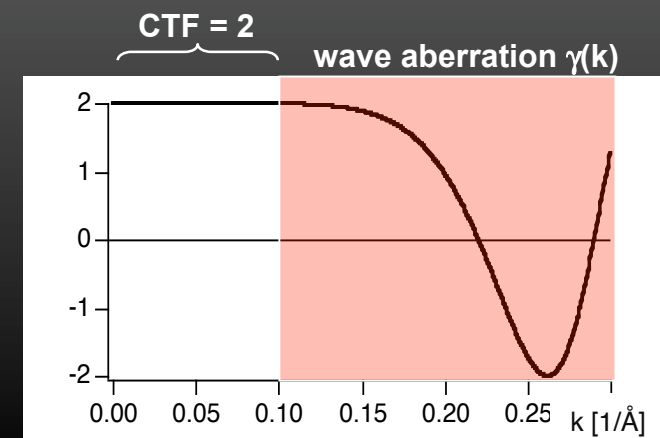
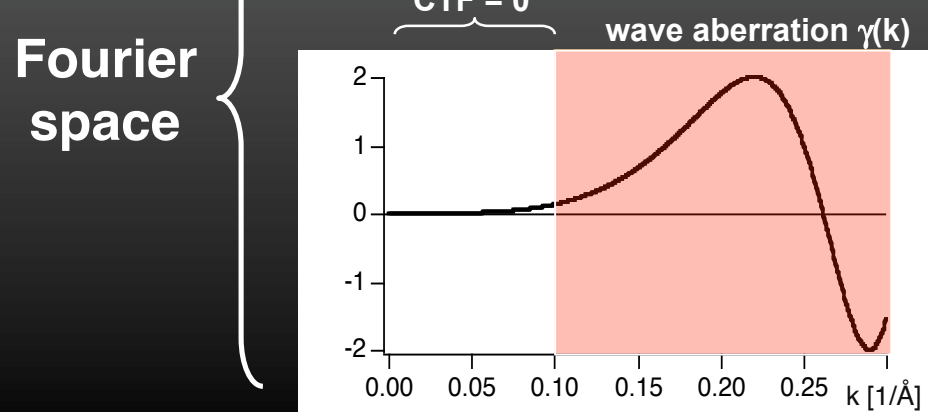


with phase plate



$\pi/2$ -phase shift
→
phase plate

Fourier space
 $\text{CTF}(k) = \text{Contrast Transfer Function } (k = \text{spatial frequency})$
 $\text{CTF}(k) = 2 \sin \gamma(k)$ → $\text{CTF}_{\pi/2}(k) = 2 \cos \gamma(k)$

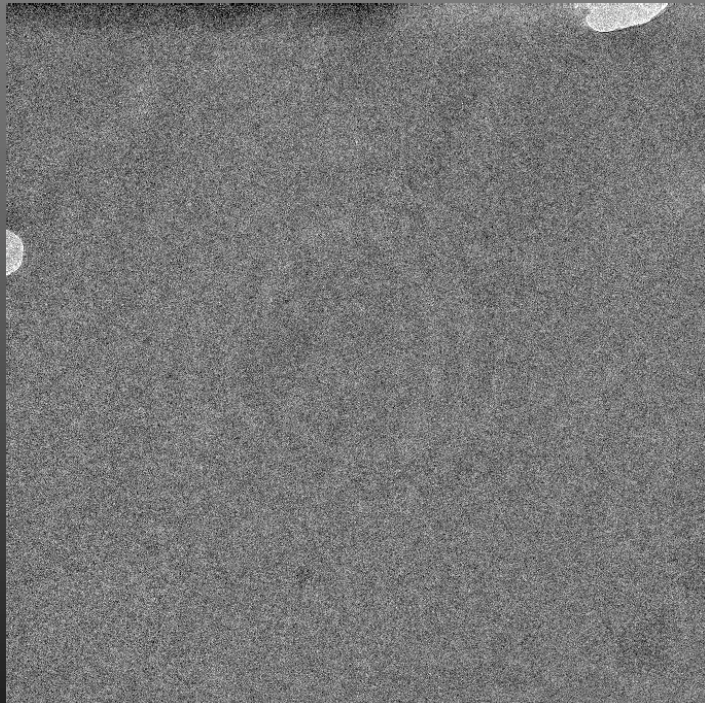


C. elegans Cell Section

High pressure frozen, freeze substituted without stain (Martin Müller)

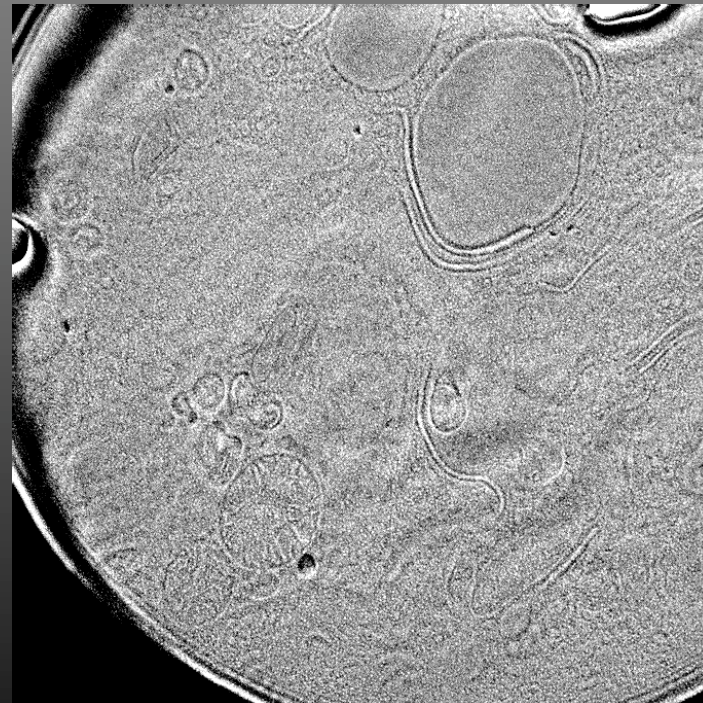
Images taken at 300keV, JEOL 3100 EFE at 4K specimen temperature
(Kuniaki Nagayama)

conventional bright field



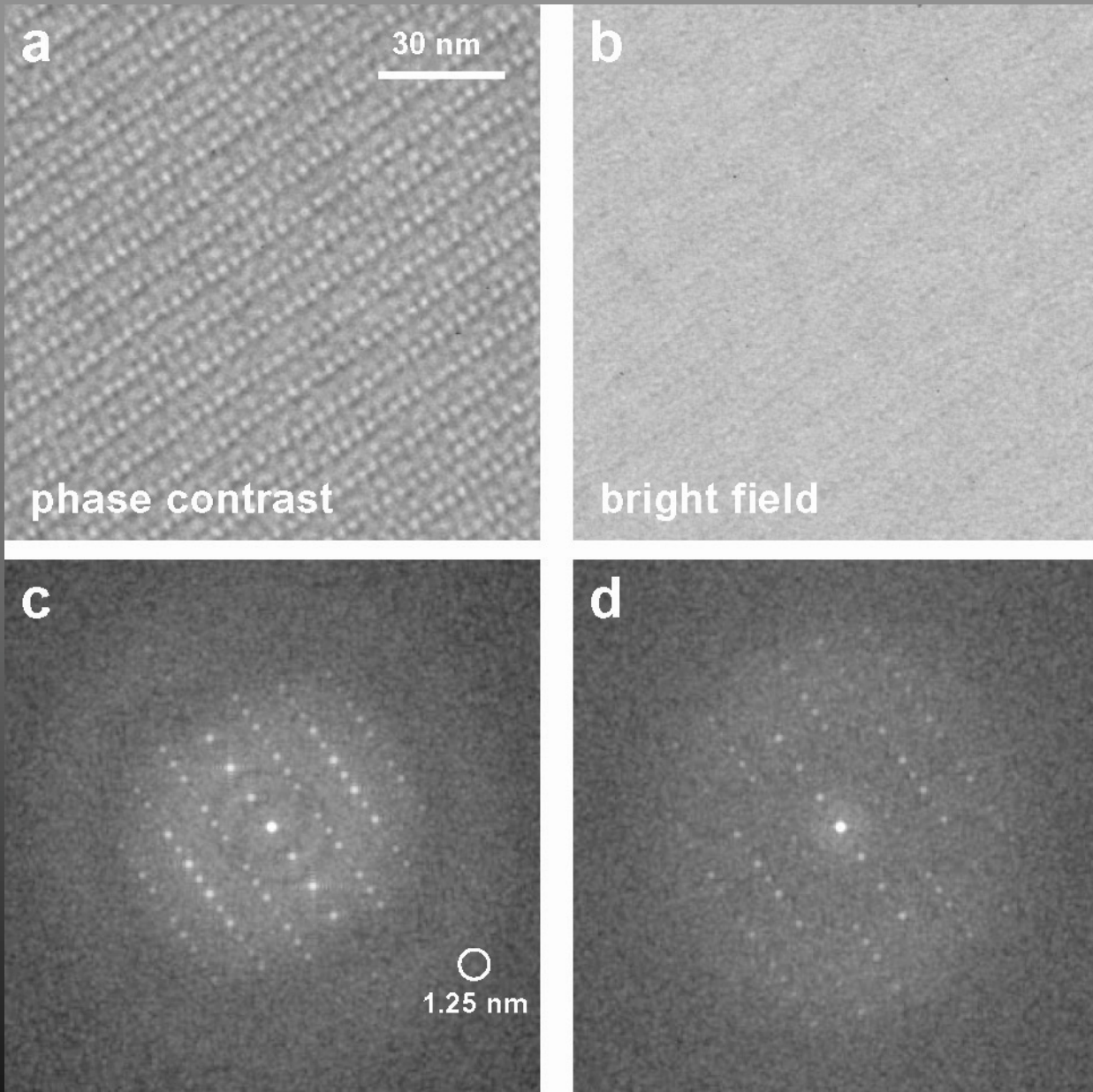
(field of view 50μm x 50μm)

Zernike phase contrast (hole in C-film)



**Catalase
protein crystal
(ice embedding)**

Zeiss-NTS 922
FEG EFTEM

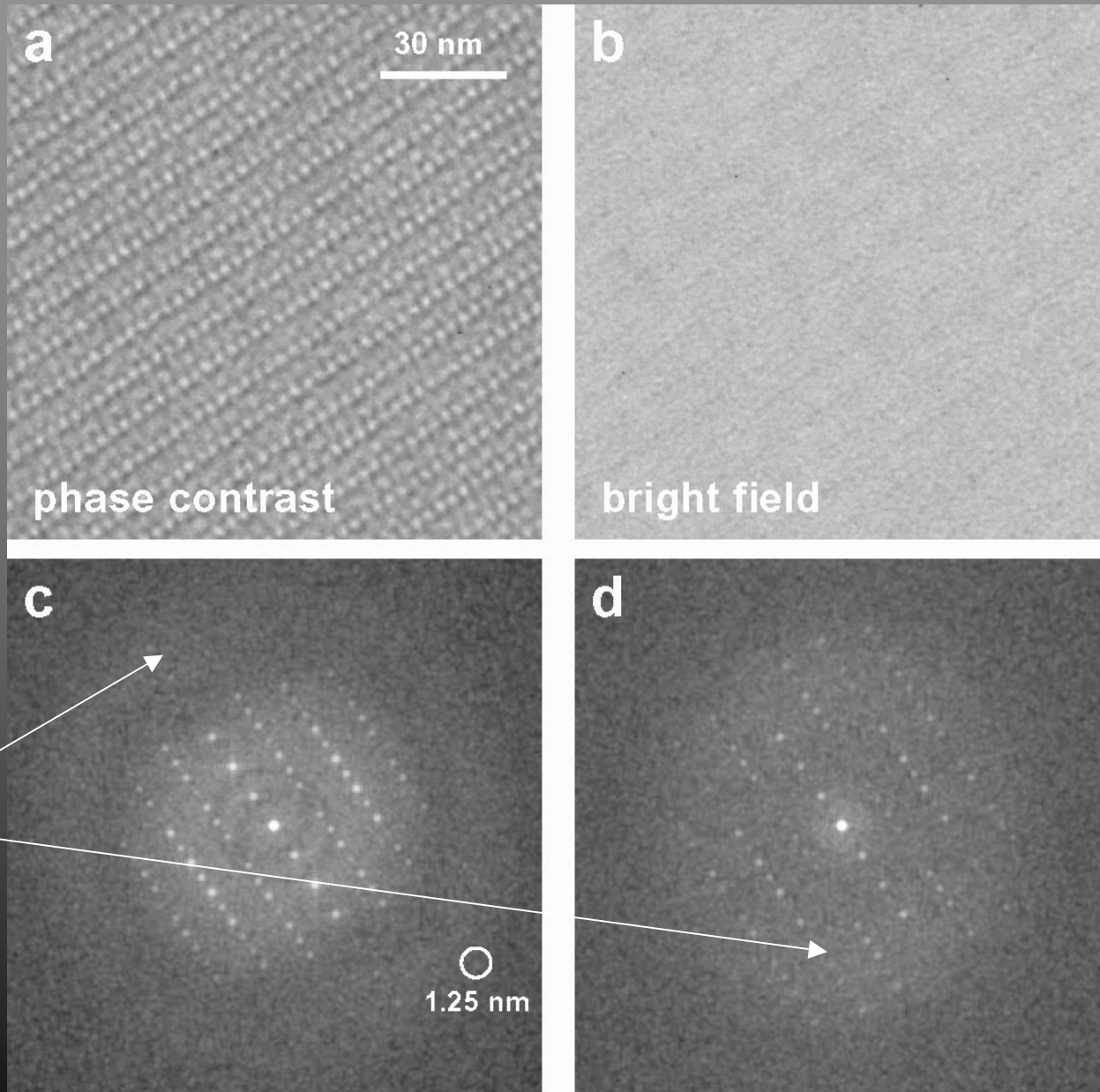


power spectra

**Catalase
protein crystal
(ice embedding)**

Zeiss-NTS 922
FEG EFTEM

Thon rings =
show directly
the $|CTF|^2$



images

power spectra

Transfer function and wave aberration

without phase plate

$$CTF \sim -2 \sin\left(\frac{\pi}{2} (C_s \lambda^3 k^4 - 2 \Delta_z \lambda k^2)\right)$$

with phase plate

$$CTF \sim -2 \sin\left(\frac{\pi}{2} (C_s \lambda^3 k^4 - 2 \Delta_z \lambda k^2) + \varphi(k)\right)$$

+90° phase shift

$$CTF \sim -2 \cos\left(\frac{\pi}{2} (C_s \lambda^3 k^4 - 2 \Delta_z \lambda k^2)\right)$$

**C_s correction
(spherical aberration)**

$$CTF \sim -2 \cos\left(\frac{\pi}{2} (0 - 2 \Delta_z \lambda k^2)\right)$$

in focus

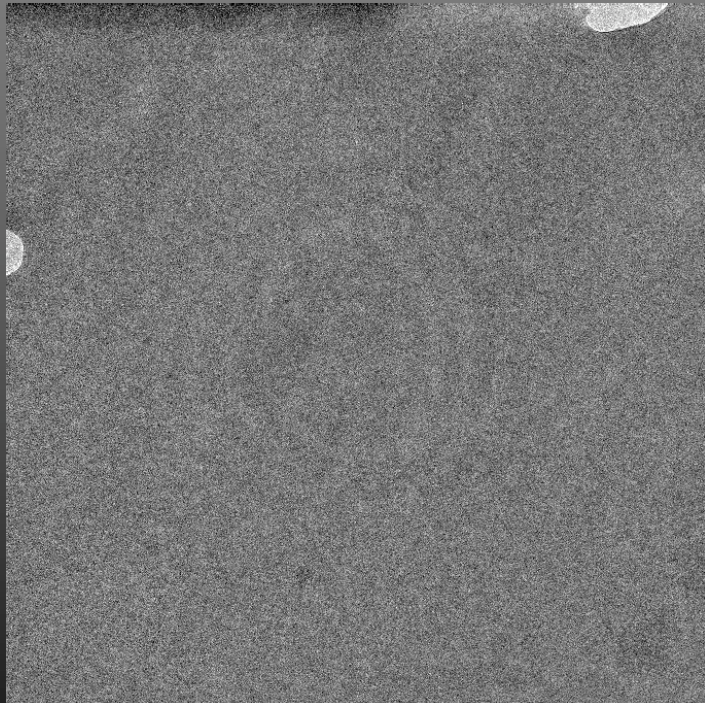
$$CTF \sim -2 \cos\left(\frac{\pi}{2} (0 - 0)\right) = 2 \cos 0 = 2$$

C. elegans Cell Section

High pressure frozen, freeze substituted without stain (Martin Müller)

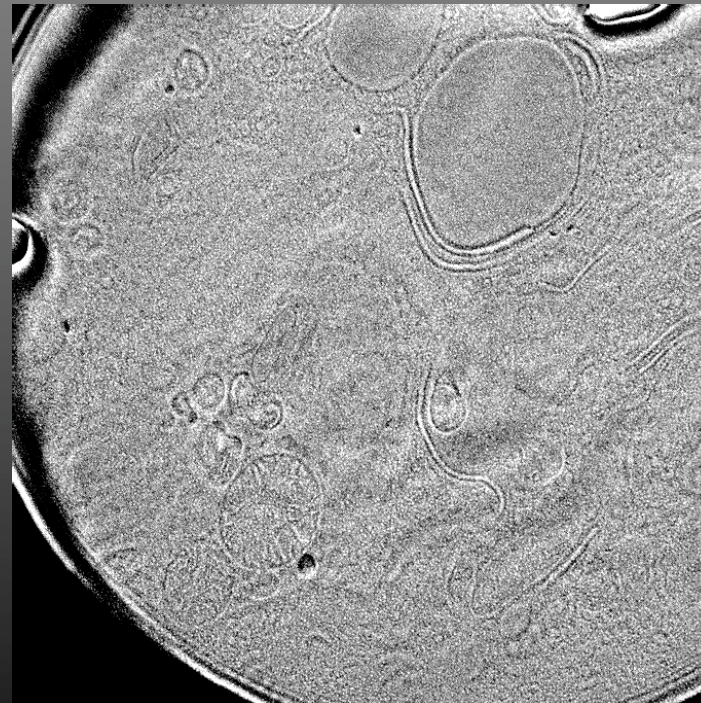
Images taken at 300keV, JEOL 3100 EFE at 4K specimen temperature
(Kuniaki Nagayama)

conventional bright field



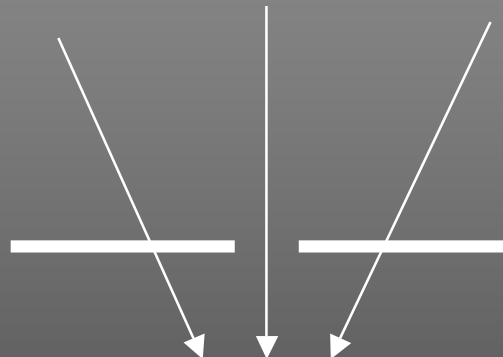
(field of view 50μm x 50μm)

Zernike phase contrast (hole in C-film)

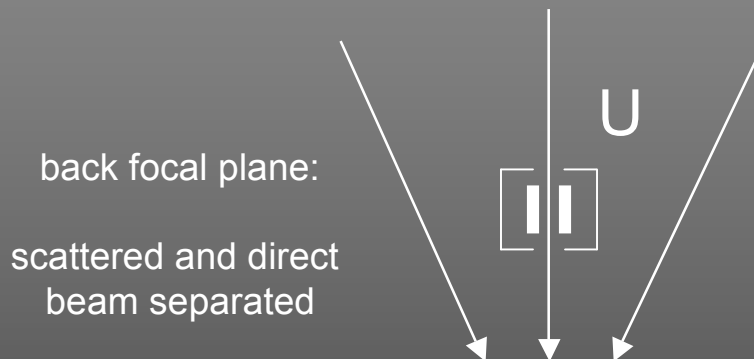


Two Types of Phase Plates

Zernike



Boersch



- phase shift of scattered electrons by inner potential of carbon film
- loss of coherence
- granularity \Rightarrow non-constant phase shift
- contamination \Rightarrow charging

back focal plane:
scattered and direct
beam separated

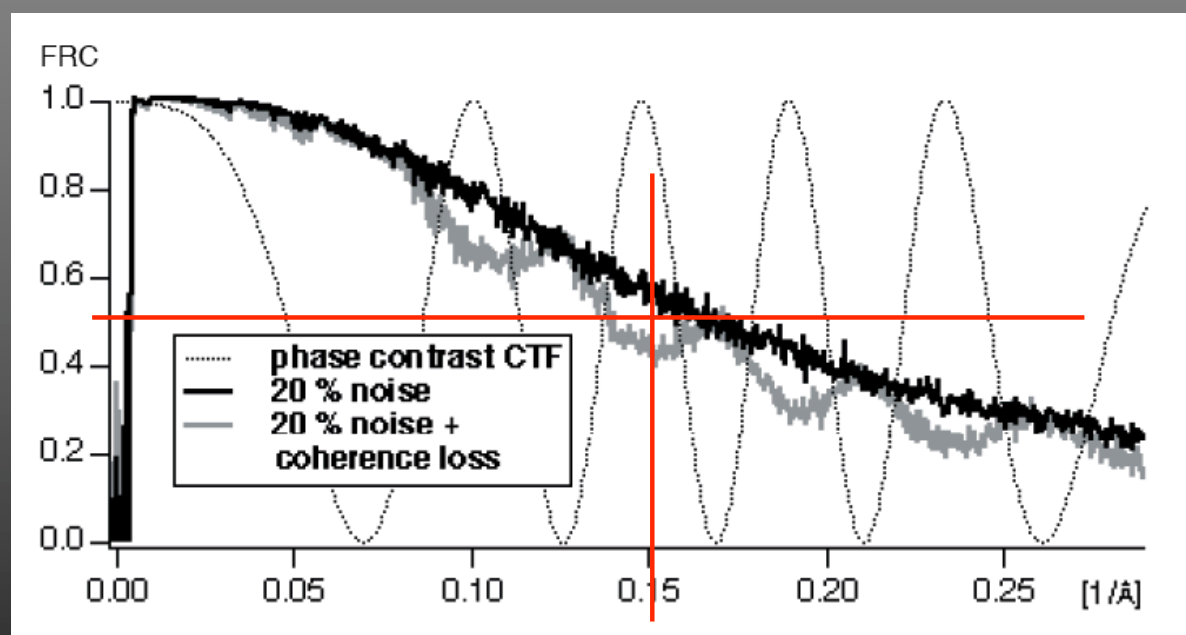
- phase shift of central beam by electrostatic potential
- no interaction with matter
- adjustable potential / phase shift
- no contamination

Measure resolution as a function of noise and coherence loss by Zernike-type thin film phase plate

original



Fourier ring correlation



simulated phase
contrast image

resolution limit 6-8 Å
cmp: 2-3 Å by electron crystallography

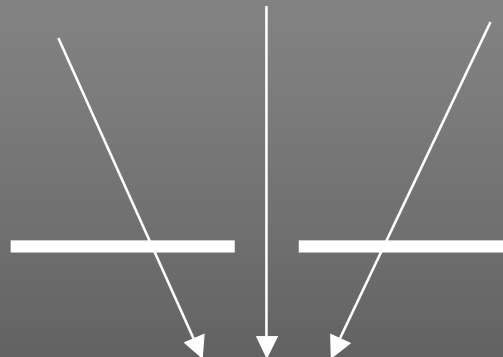
Majorovits and RRS, unpublished

Prerequisites for ideal phase plate

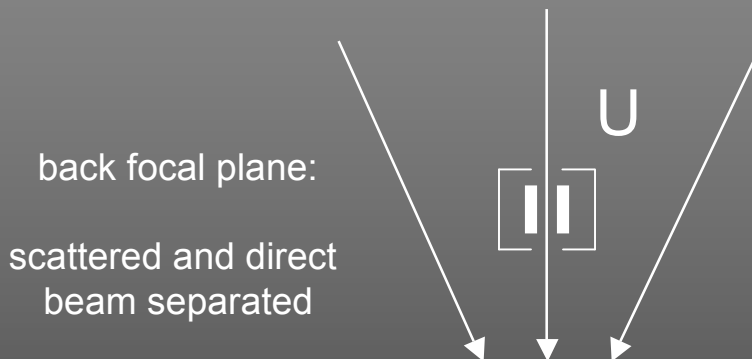
- phase shift by magnetic or electric field
 - > no additional scattering
- no other effects than homogeneous phase shift
 - > non-homogeneous effects (lens)
 - > obstructions in the back focal plane

Two Types of Phase Plates

Zernike



Boersch

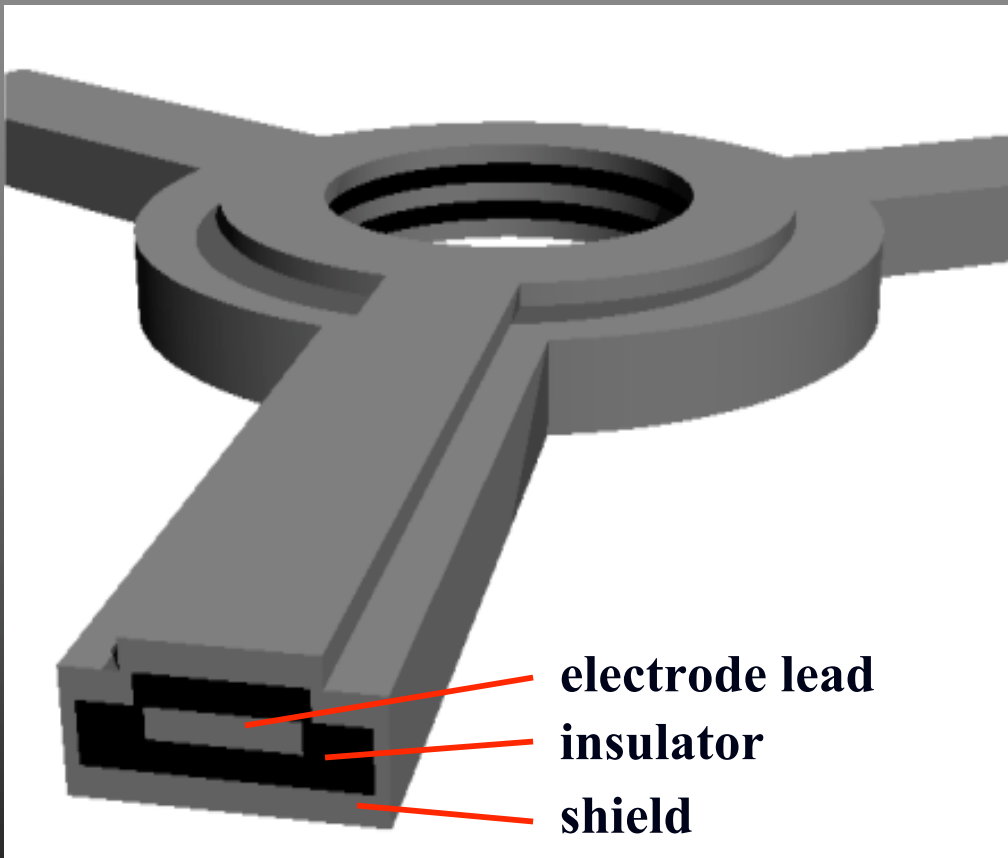


- phase shift of scattered electrons by inner potential of carbon film
- loss of coherence
- granularity \Rightarrow non-constant phase shift
- contamination \Rightarrow charging

back focal plane:
scattered and direct
beam separated

- phase shift of central beam by electrostatic potential
- no interaction with matter
- adjustable potential / phase shift
- no contamination

Design of the Boersch Phase Plate



- Realization of an electrostatic microlens by a five-layered electrode structure in the center of the phase plate
- Confinement of the electrical field to the central lens opening by surrounding Au layer

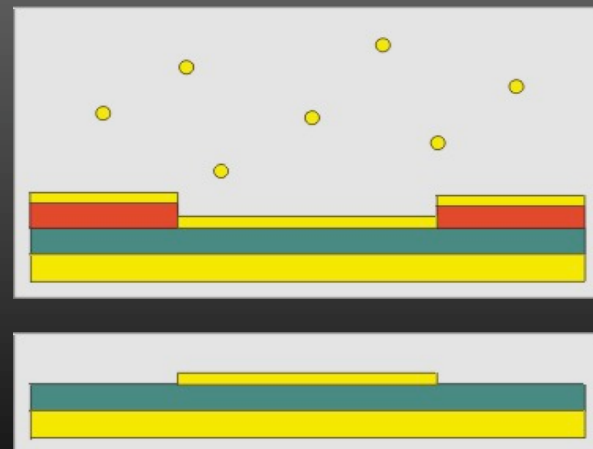
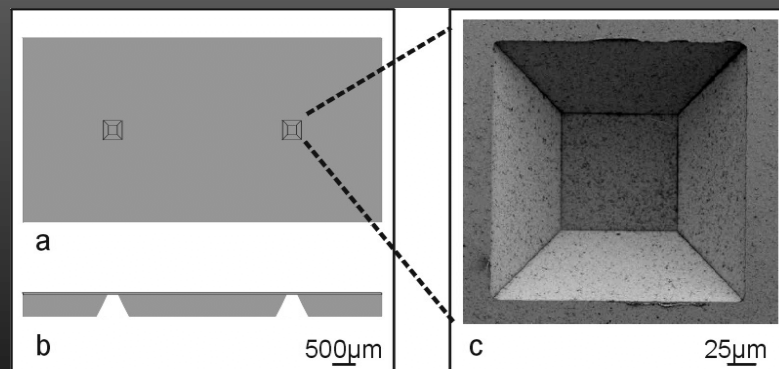
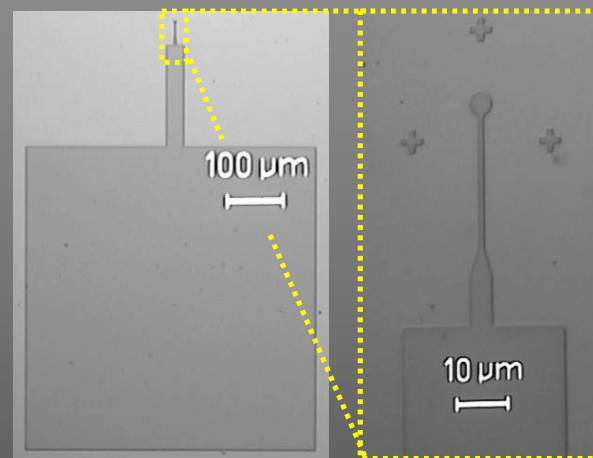
Matsumoto and Tonomura, Ultramicroscopy, 63 (1996)

Schultheiß et al., J. Instrum. Res. 77 (2006)

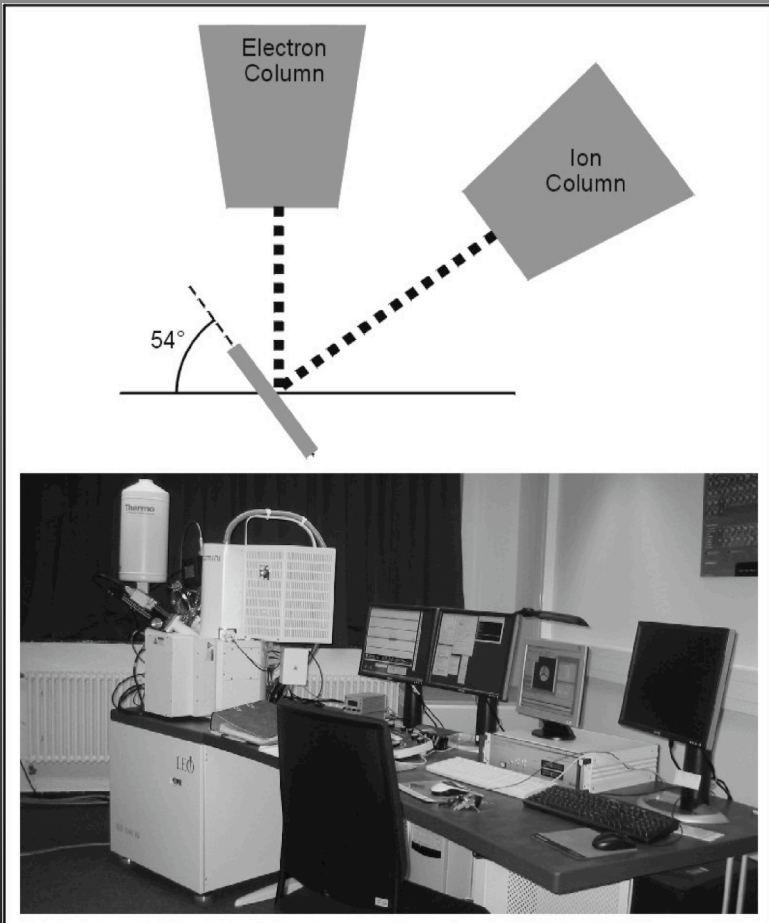


Substrate Material / Lower 3 Layers

- Commercially available low-stress $\text{Si}_{3+x}\text{N}_{4-x}$ membranes as basic material
- Electron-beam evaporation of the lower shielding Au layer
- Patterning of the electrode layer by electron-beam lithography

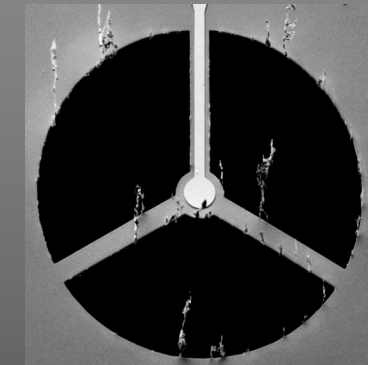


Focused Ion Beam (FIB) Lithography

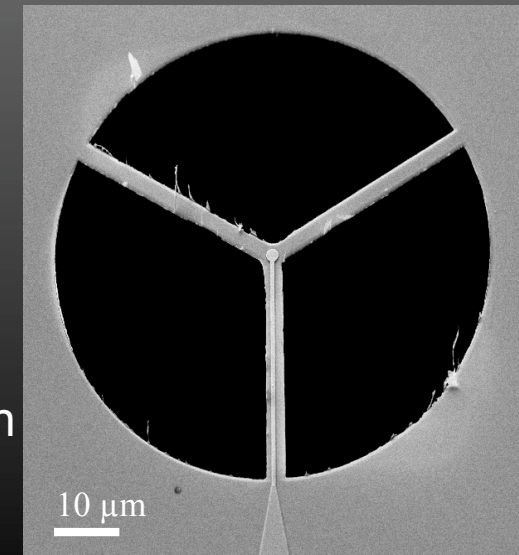


- Shaping of phase plate by FIB lithography

First tested design

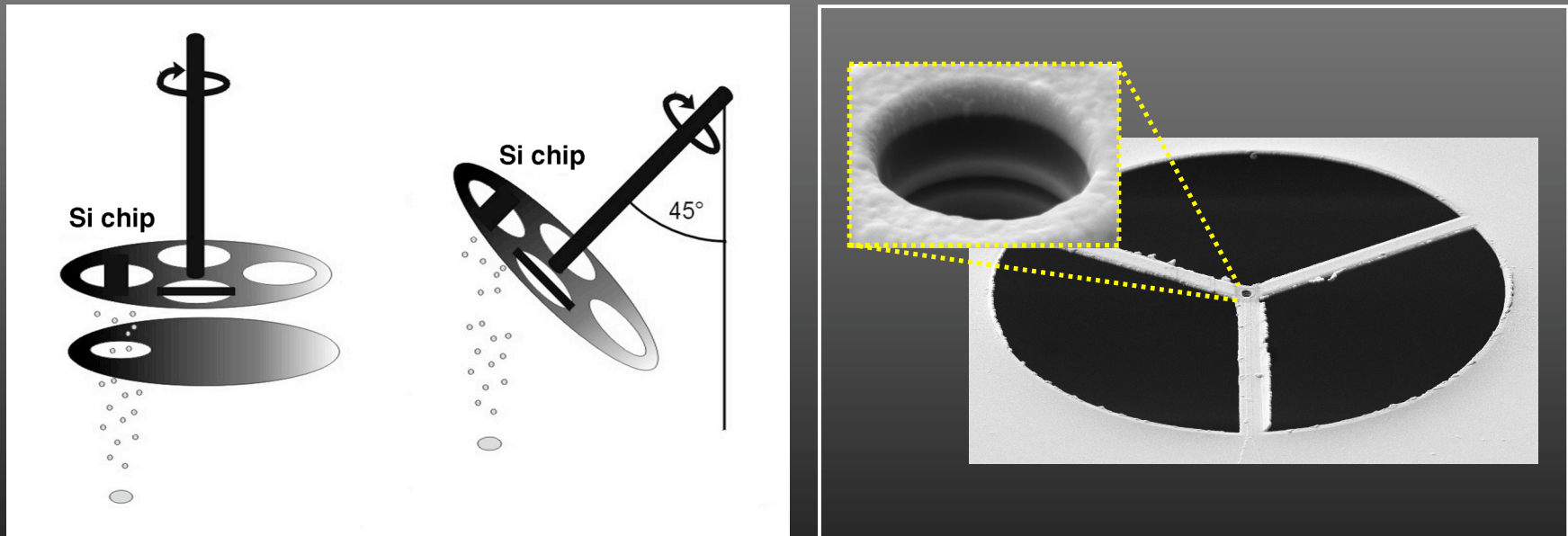


Improved design with reduced supporting bar width



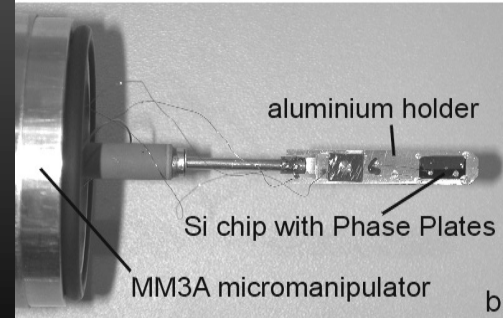
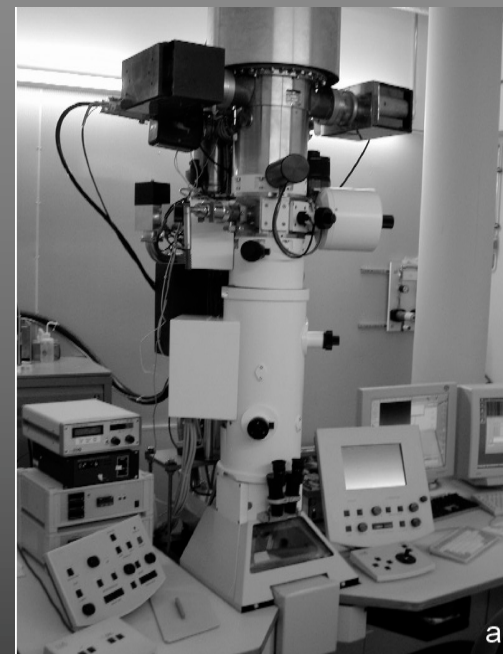
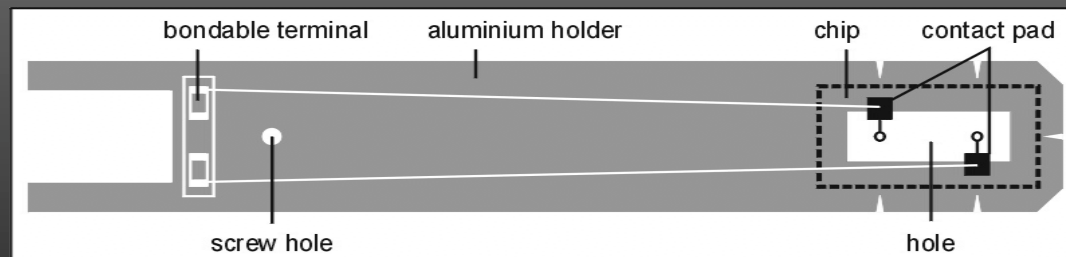
Shielding Layer / Central Hole

- Electron-beam evaporation of 2nd insulating layer (Al_2O_3)
- Electron-beam evaporation of shielding gold layer in tilted rotating holder
- Central lens opening by FIB milling



Connection and Implementation

- Chip glued on an aluminium holder
- Mounting of aluminium holder on a piezodriven micro manipulator to position the phase plate in the back focal plane
- Electrical bushing through flange



Transfer function and wave aberration

without phase plate

$$CTF \sim -2 \sin\left(\frac{\pi}{2} (C_s \lambda^3 k^4 - 2 \Delta_z \lambda k^2)\right)$$

with phase plate

$$CTF \sim -2 \sin\left(\frac{\pi}{2} (C_s \lambda^3 k^4 - 2 \Delta_z \lambda k^2) + \varphi(k)\right)$$

+90° phase shift

$$CTF \sim -2 \cos\left(\frac{\pi}{2} (C_s \lambda^3 k^4 - 2 \Delta_z \lambda k^2)\right)$$

**C_s correction
(spherical aberration)**

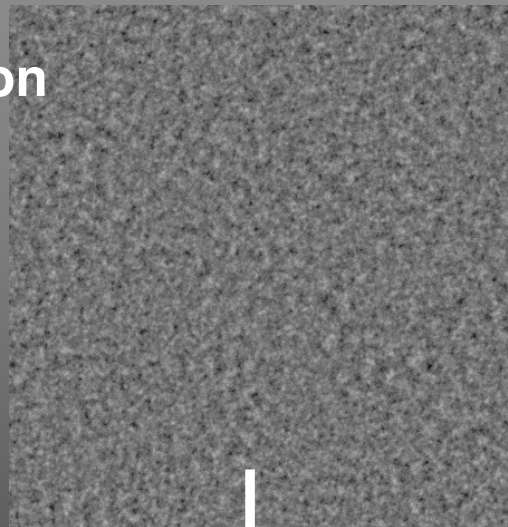
$$CTF \sim -2 \cos\left(\frac{\pi}{2} (0 - 2 \Delta_z \lambda k^2)\right)$$

in focus

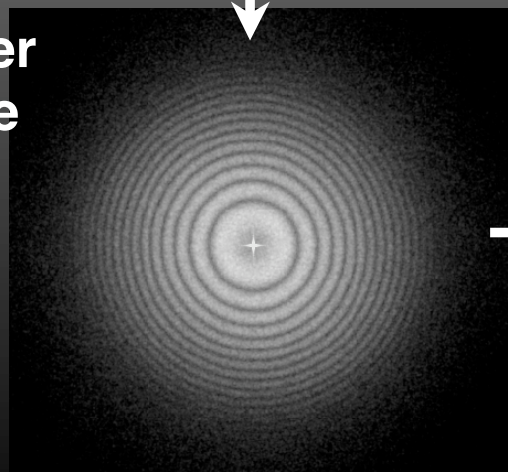
$$CTF \sim -2 \cos\left(\frac{\pi}{2} (0 - 0)\right) = 2 \cos 0 = 2$$

Quantitation of phase shift using carbon film

carbon
film

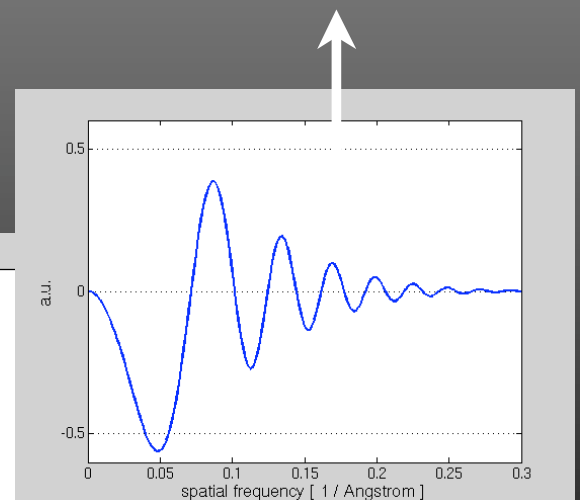
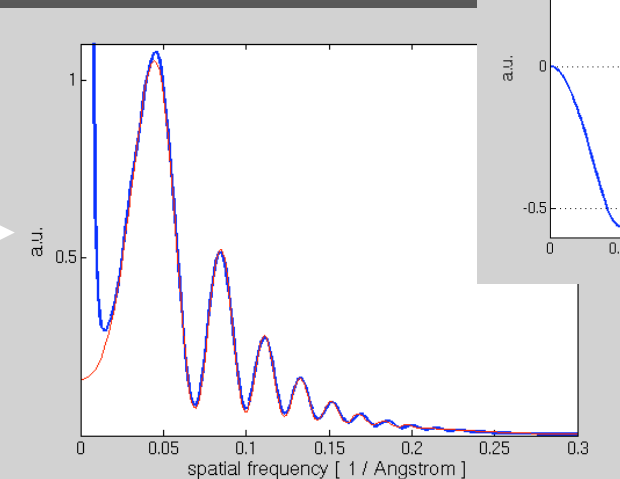


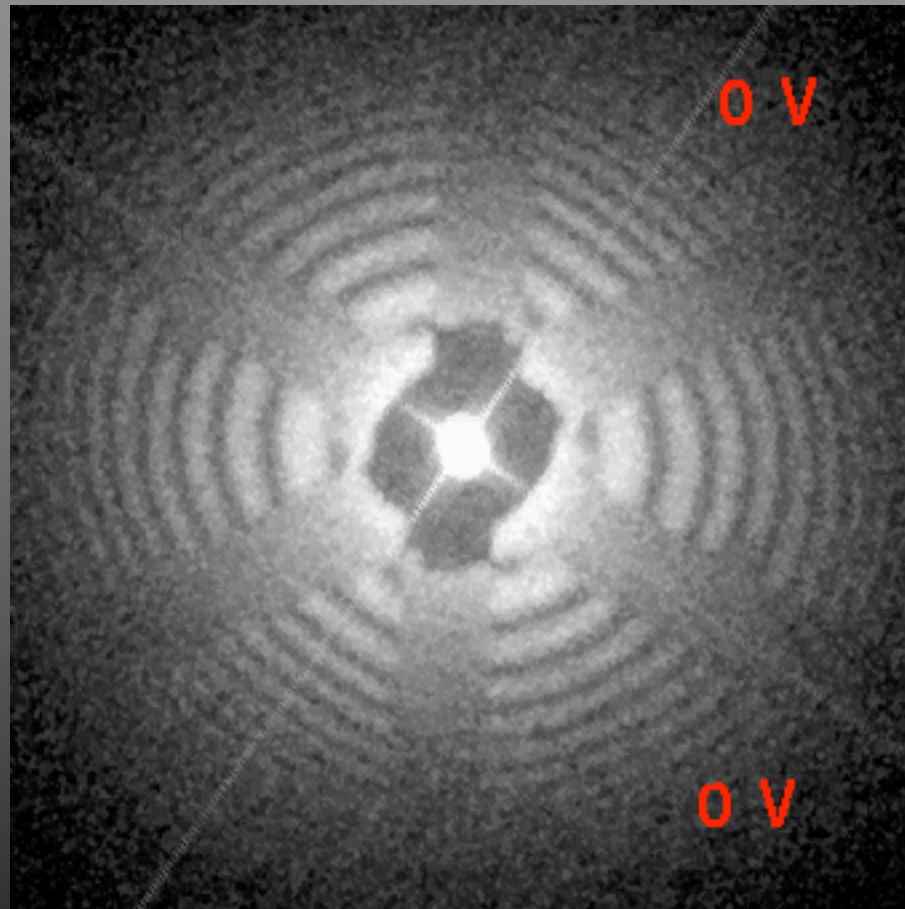
Fourier
space

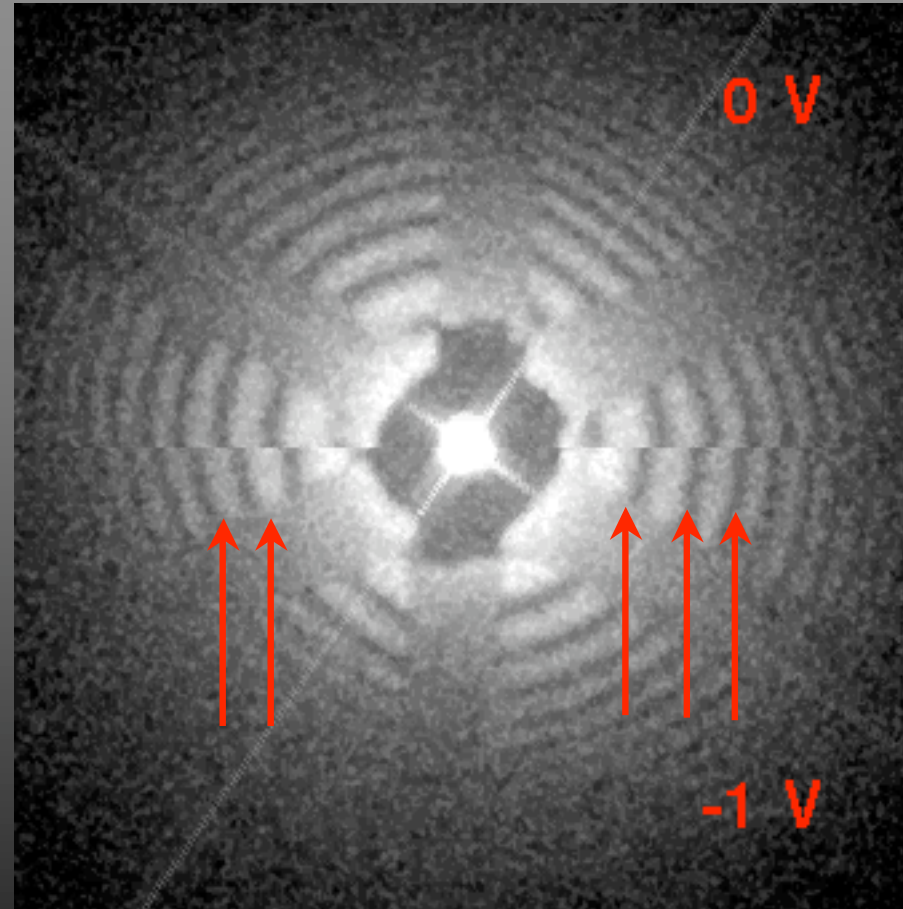


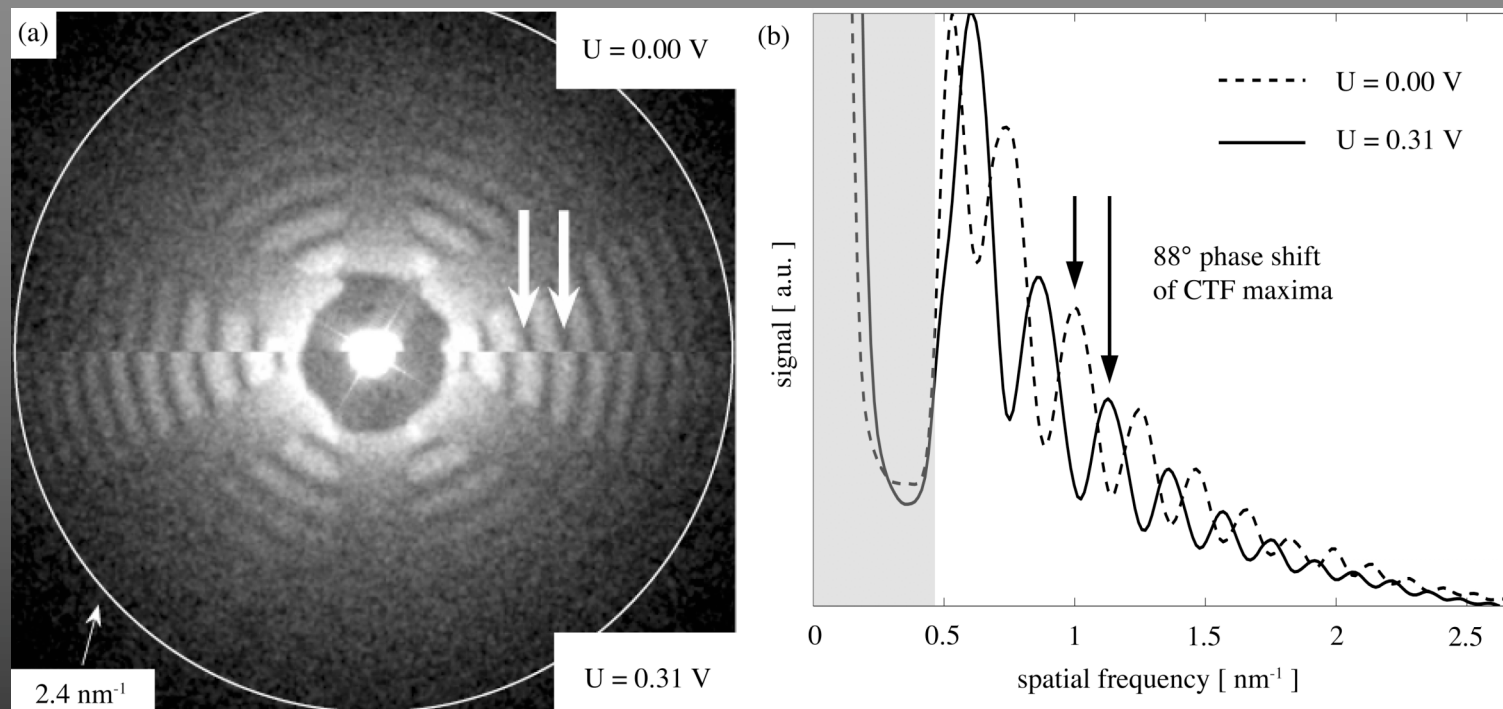
$$CTF \sim -2 \sin\left(\frac{\pi}{2} \left(C_s \lambda^3 k^4 - 2 \Delta \zeta \lambda k^2 \right) + \varphi(k) \right)$$

$\varphi(k)$ = phase shift



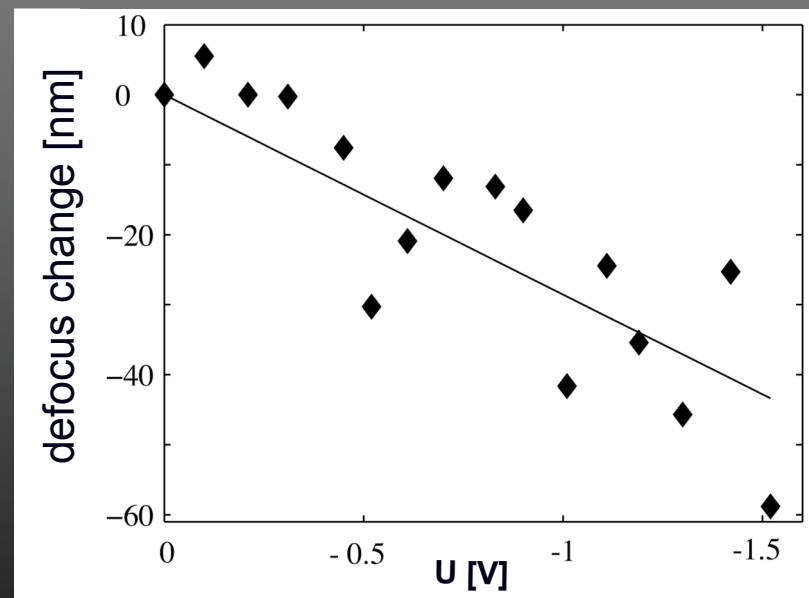
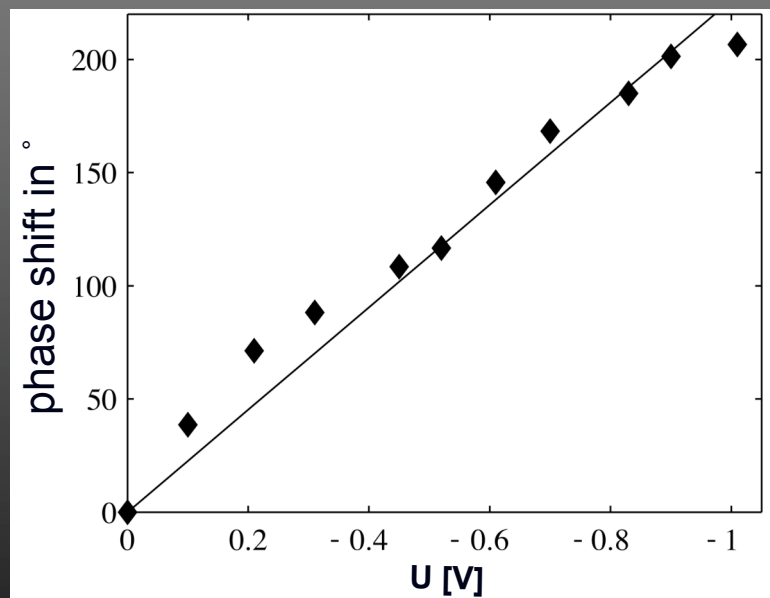




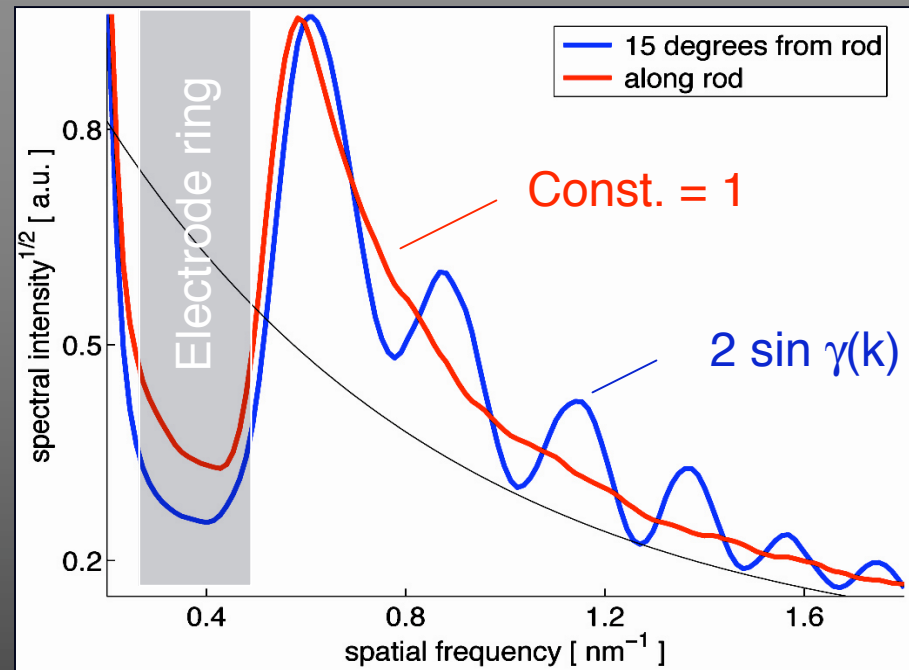
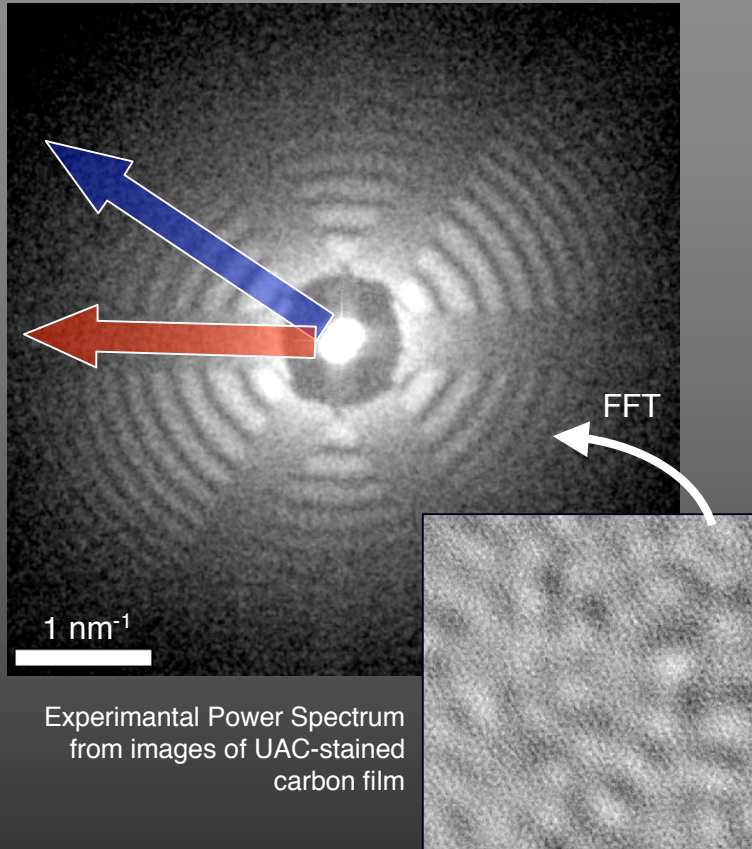


It works!

- realisation of an electrostatic Boersch phase plate
- proof of principle of high resolution PCEM



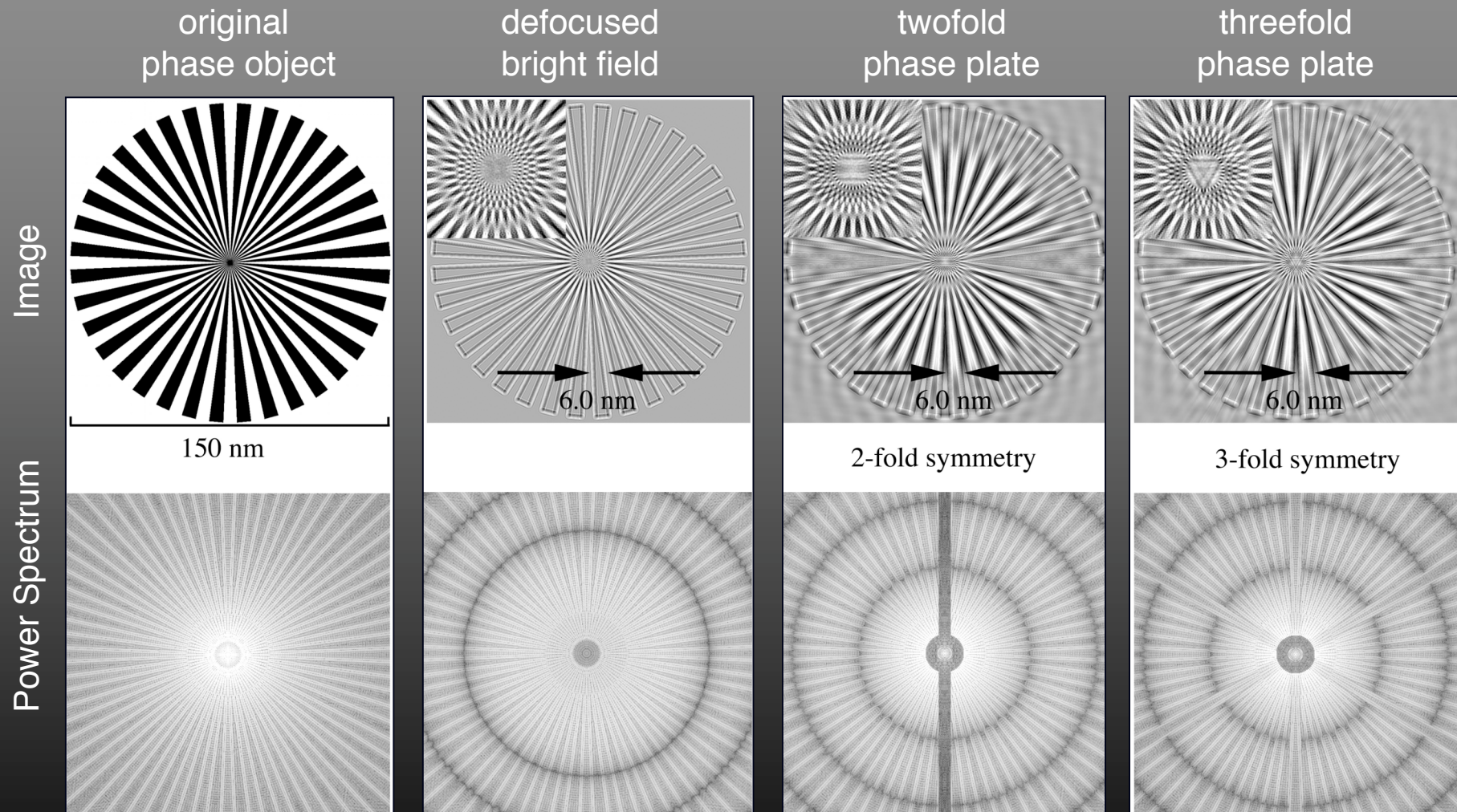
Measurement of Signal Transfer „Along“ Support Rod



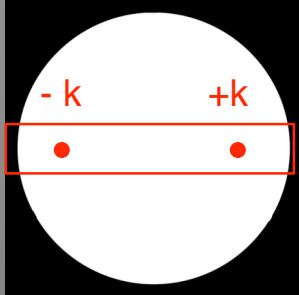
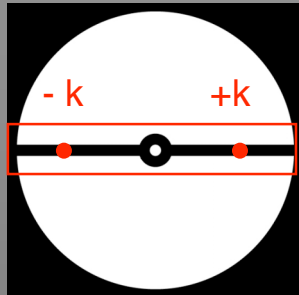
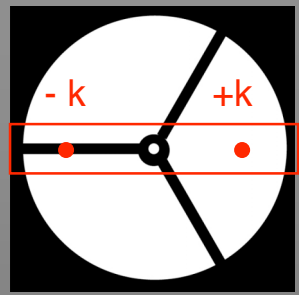
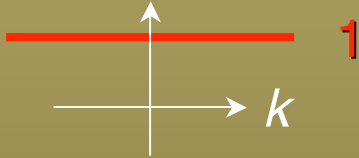
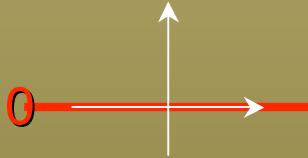
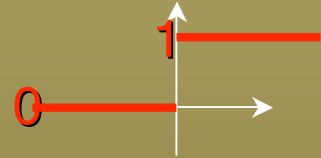
Radial intensity of power spectrum shown on right side
= Single-sideband signal vs. Bright field signal

→ Non-oscillating single-sideband signal transfer by
non-centrosymmetric support rods

Threefold Support Symmetry Preserves Object Information and Reduces Imaging Artifacts

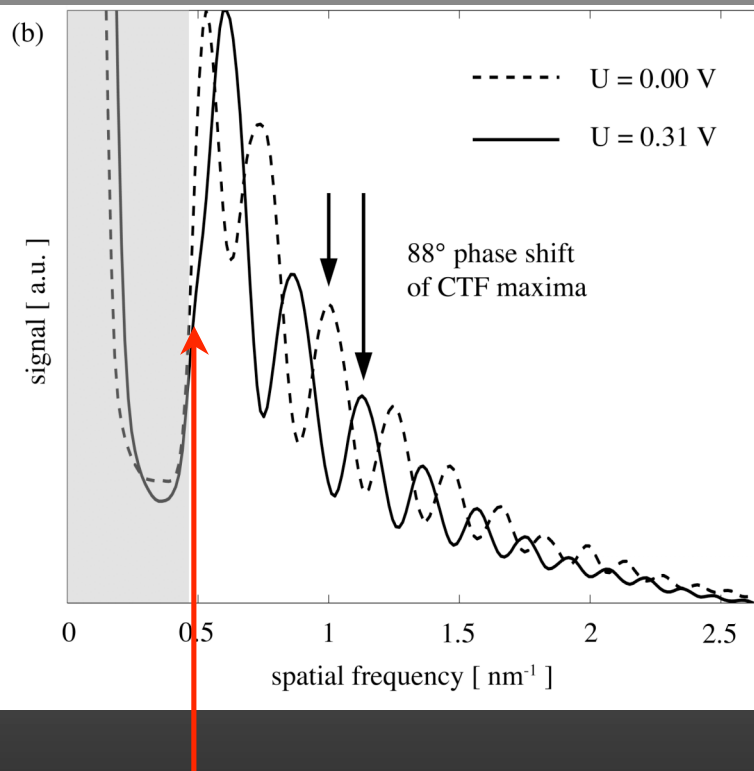
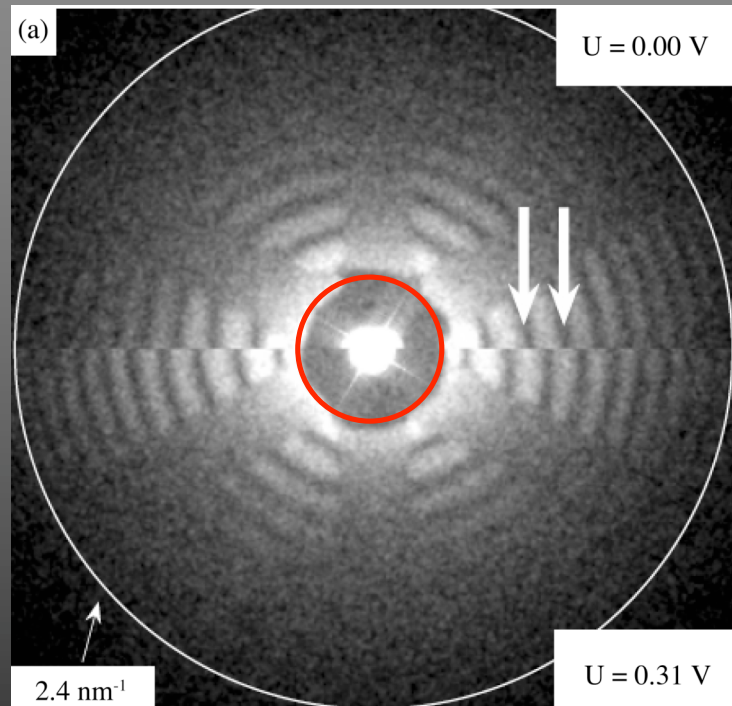


Simulation: Imaging of a weak phase object (Siemens star) with 120 kV TEM

	no phase plate	twofold PP	threefold PP
Support geometry			
Phase Plate aperture function $A(k)$ in back focal plane (in rod direction)	 One $A_0(k) = 1$	 Zero $A_2(k) = 0$	 Heaviside step function $A_3(k) = 1/2 \{ 1 + sign(k) \}$
Wave amplitude in BFP	$\delta(k) + i \varphi(k) \bullet e^{-i W(k)}$	$\delta(k)$	$\delta(k) + i/2 \varphi(k) \bullet e^{-i W(k)} \{ 1 + sign(k) \}$
Image frequency spectrum (Fourier transform)	$\delta(k) + \varphi(k) \bullet 2 \sin W(k)$	$\delta(k)$	$\delta(k) + \varphi(k) \bullet i \underbrace{\sin(k) e^{-i sign(k) W(k)}}_{\text{PCTF = phase factor !}}$
Phase contrast transfer PCTF (k)	$2 \sin W(k) $	0	1

Another Problem:

Loss of Low Resolution Structure Factors

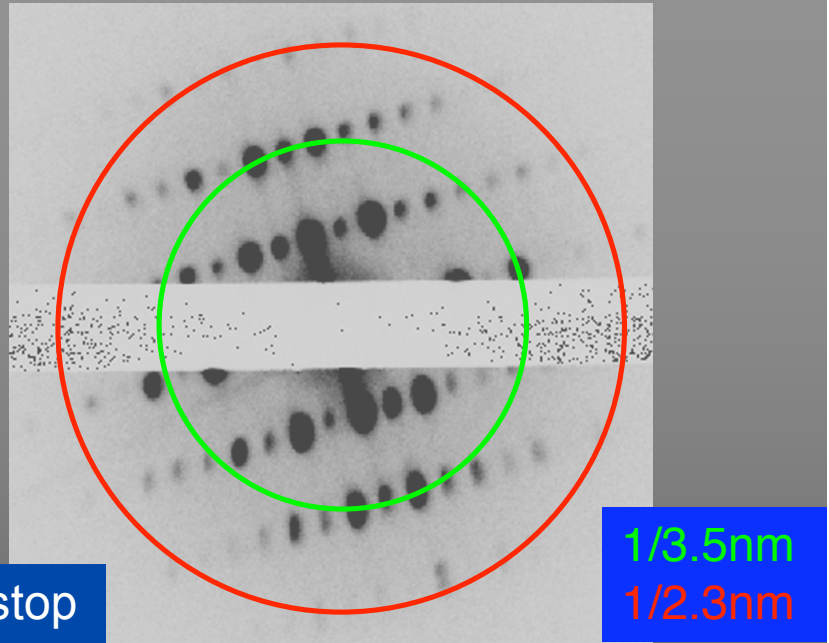


2 nm resolution ring

2 nm resolution cut-off

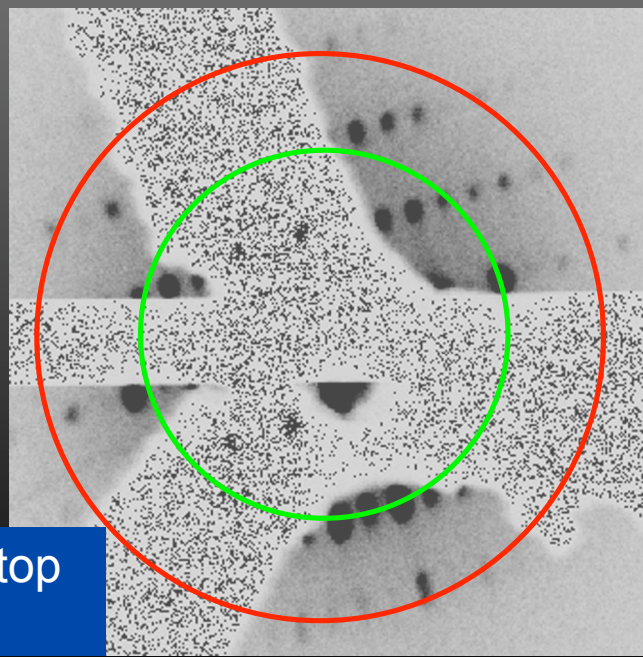
Electron diffraction patterns

(catalase micro crystals, negative stain
100keV, 3mm focal length)



Shadow of beam stop

1/3.5nm
1/2.3nm



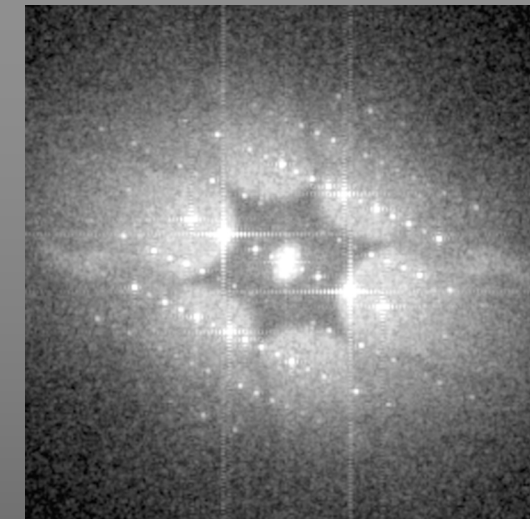
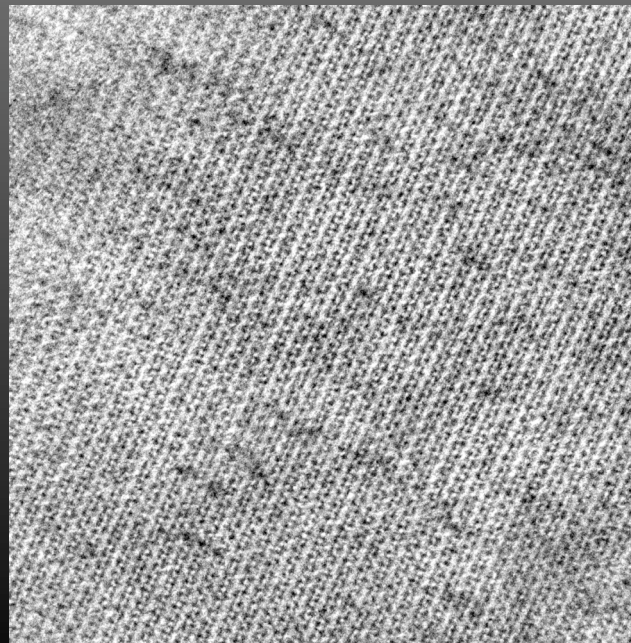
Shadow of beam stop
and phase plate

Imaging

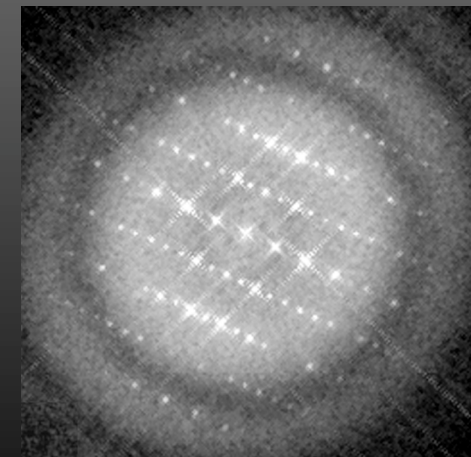
(catalase, negative
stain, 100keV,
65kx on CCD
6.9nm,17.3nm)

**with phase
plate in diff.
plane**

**conventional
bright field**



power spectra



The Roadmap to High Resolution Phase Contrast EM

Proof of principle (structure factors 2nm - 4Å)



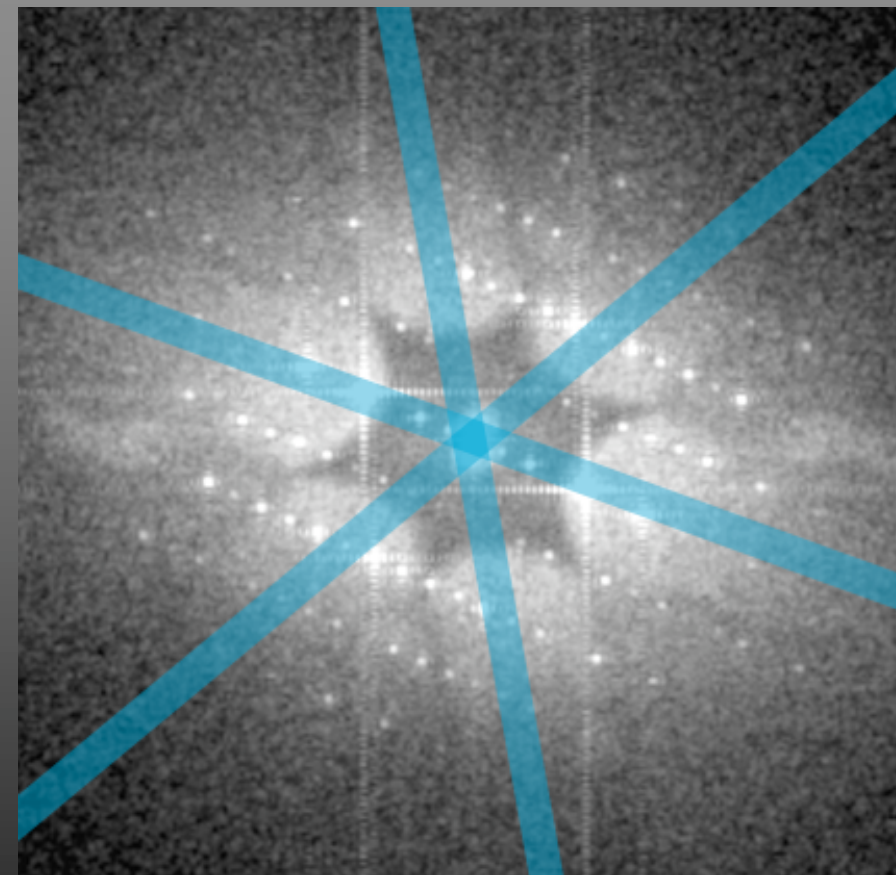
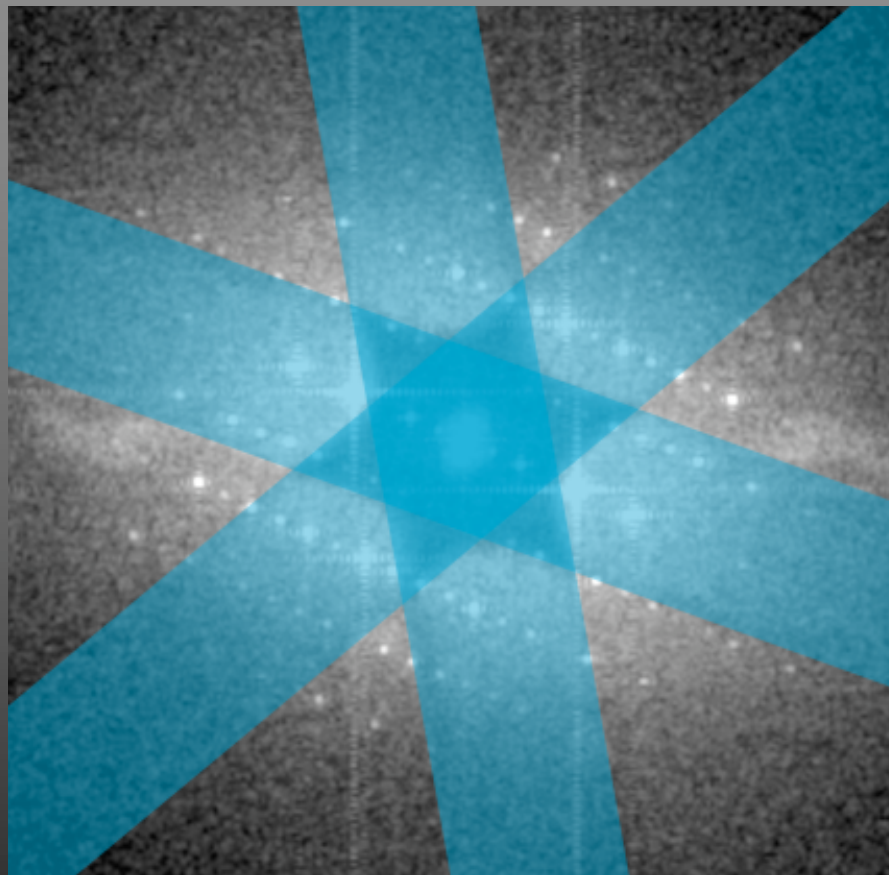
Smaller lens diameter (structure factors 4nm - 2Å) and thinner support rods



Increase effective size of diffraction pattern
(structure factors 40nm - 2Å)



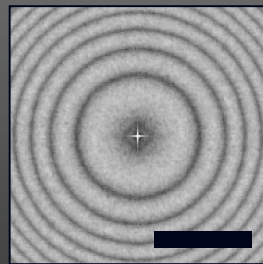
Artefact-free imaging of objects of typical size of 20-30nm



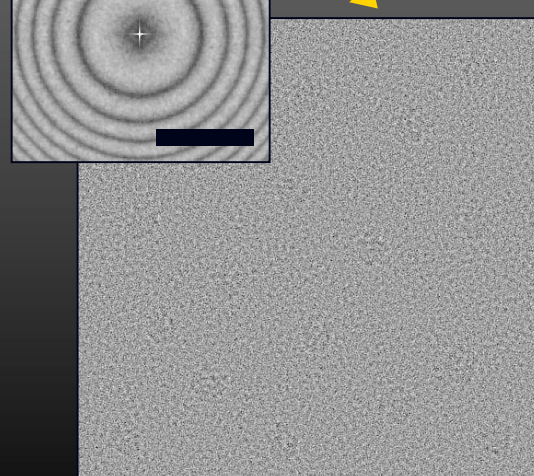
Reducing Signal Obstruction by the Phase Plate

Simulate the optical magnification
of back focal plane
(300kV, focal length 2.2mm)

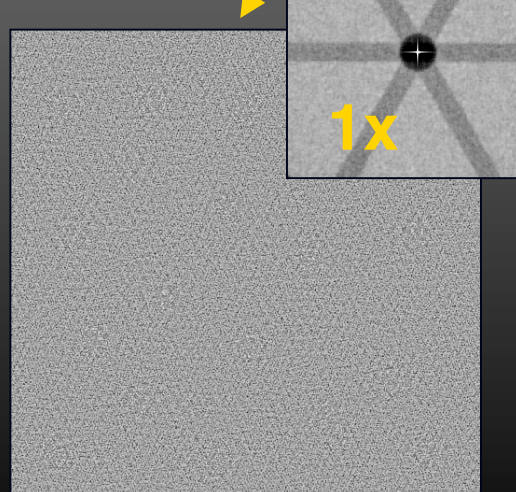
Bright Field
 $1 \mu\text{m}$ underfocus



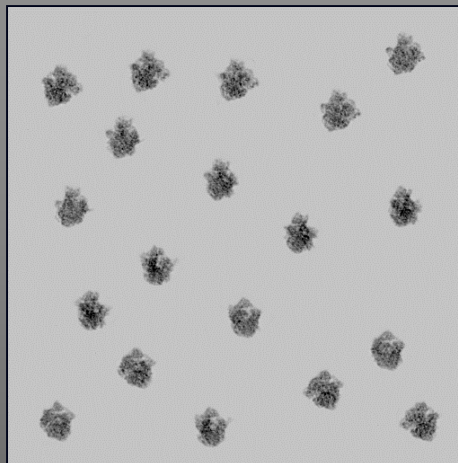
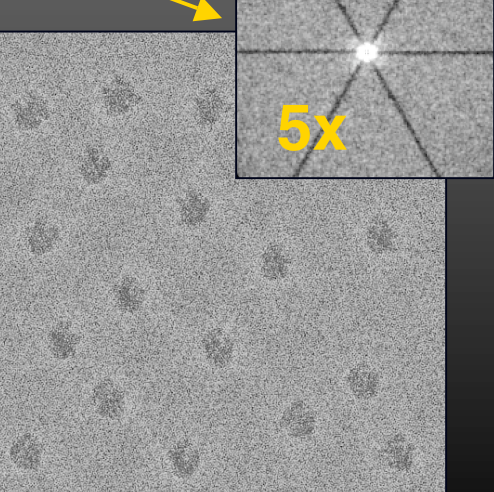
SNR = 0.61



SNR = 0.68



SNR = 1.64



Test object: field of different ribosome projections (from PDB) with simulated ice embedding

100 nm

3-fold Boersch Phase Plate, in gaussian focus

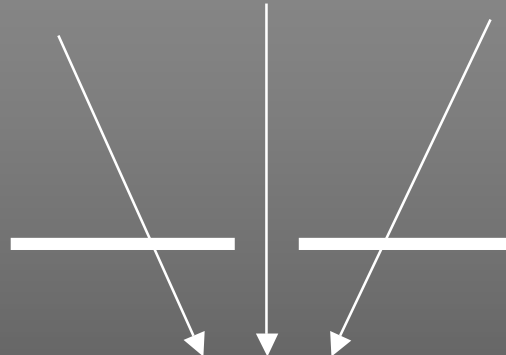
Conclusion and future work

- phase shift by electric field shown (proof of principle)
 -> no additional scattering
 - no other effects than homogeneous phase shift
 -> non-homogeneous effects (lens)
 -> obstructions in the back focal plane
- > Design and construct a lens doublet to magnify
 the back focal plane
 (problems with spherical aberration, resolution ...)

Majorovits et al., Ultramicroscopy, in press (2006 or 2007)
on the web under: doi 10.1016/j.ultramic.2006.7.006

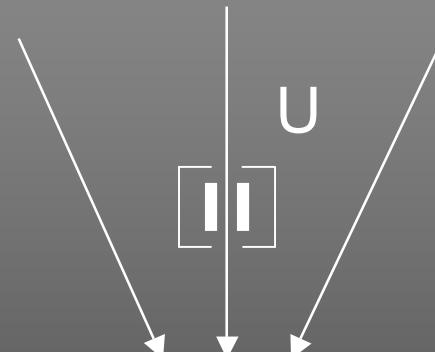
Two Types of Phase Plates

Thin-film Zernike



Fritz Zernike

Boersch



Hans Boersch